Report No. K-TRAN: KU-00-11
FINAL REPORT

Field Instrumentation and Monitoring of Kansas Department of Transportation Fiber Composite Bridge for Long Term Behavior Assessment

Jeffry S. Adams
Guillermo Ramirez, Ph.D.
JoAnn Browning, Ph.D.

University of Kansas
Lawrence, Kansas

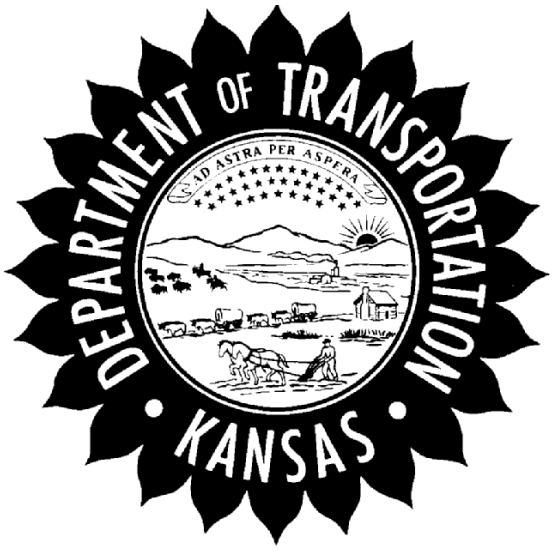

APRIL 2005

K-TRAN

A COOPERATIVE TRANSPORTATION RESEARCH PROGRAM BETWEEN:
KANSAS DEPARTMENT OF TRANSPORTATION
KANSAS STATE UNIVERSITY
THE UNIVERSITY OF KANSAS

1 Report No. K-TRAN: KU-00-11	2 Government Accession No.	3 Recipient Catalog No.
4 Title and Subtitle FIELD INSTRUMENTATION AND MONITORING OF KANSAS DEPARTMENT OF TRANSPORTATION FIBER COMPOSITE BRIDGE FOR LONG-TERM BEHAVIOR ASSESSMENT		5 Report Date April 2005 6 Performing Organization Code
7 Author(s) Jeffry S. Adams*, Guillermo Ramirez, Ph.D.*, and JoAnn Browning, Ph.D. *affiliated with Performing Organization at time of research.		8 Performing Organization Report No.
9 Performing Organization Name and Address University of Kansas 1530 W. 15th Street Lawrence, Kansas 66045		10 Work Unit No. (TRAIS) 11 Contract or Grant No. C1163
12 Sponsoring Agency Name and Address Kansas Department of Transportation Bureau of Materials and Research 700 SW Harrison Street Topeka, Kansas 66603-3754		13 Type of Report and Period Covered Final Report August 1999 – October 2004 14 Sponsoring Agency Code RE-0208-01

15 Supplementary Notes

For more information write to address in block 9.

16 Abstract

This paper discusses results from an analytical study concerning the long-term evaluation of two fiber-reinforced polymer composite bridges in Kansas. A background on current non-destructive evaluation methodologies for monitoring structural systems and typical sensors that are used with non-destructive evaluation techniques is discussed. The results of the finite element models of the bridges are presented. A procedure for selecting and installing appropriate systems for non-destructive evaluation of the fiber-reinforced polymer composite bridges is described.

The purpose of this paper is to address specific questions proposed by the Kansas Department of Transportation regarding the performance of fiber-reinforced polymer composite decks installed in the fall of 1999 on two existing bridges, and to identify possible long-term performance problems. The main objectives are:

- To determine if composite action develops between the fiber-reinforced polymer composite deck, saddle and steel girder. And if composite action does develop, estimate the improved capacity of the bridge.
- To determine if vibration of the bridge may lead to structural deterioration.
- To evaluate the effectiveness of the bolted connections.

The data collected from the non-destructive testing on the bridge suggests that composite action may not exist. The dissipation of energy recorded using accelerometers demonstrates that the fiber-reinforced polymer composite deck and steel girder behave independently. However, studies using finite element analyses show that composite action can develop if bonded.

There is excessive vibration within the fiber-reinforced polymer deck. The results of non-destructive testing performed on one bridge showed that the deck dissipates energy in a wide frequency range. This type of energy dissipation is typically a result of excessive vibration and excitation. This is a concern and further investigation is recommended.

From the finite element analyses, the stress levels under normal traffic loading are not a concern. However, the combination of loads due to thermal differential and induced vibration due to heavy trucks can produce large stresses within the bolted connections that may lead to material fatigue.

17 Key Words	18 Distribution Statement
Composite Bridges, Fiber Reinforced Polymer, Finite Element, FRP, NDT, Non-destructive Testing	No restrictions. This document is available to the public through the National Technical Information Service, Springfield, Virginia 22161

19 Security Classification (of this report)	20 Security Classification (of this page)	21 No. of pages	22 Price
Unclassified	Unclassified	111	

Form DOT F 1700.7 (8-72)

FIELD INSTRUMENTATION AND MONITORING OF KANSAS DEPARTMENT OF TRANSPORTATION COMPOSITE BRIDGE FOR LONG-TERM BEHAVIOR ASSESSMENT

Final Report

Prepared by

Jeffry S. Adams*
Guillermo Ramirez, Ph.D.*
JoAnn Browning, Ph.D.
University of Kansas

A Report on Research Sponsored By

THE KANSAS DEPARTMENT OF TRANSPORTATION
TOPEKA, KANSAS

UNIVERSITY OF KANSAS
LAWRENCE, KANSAS

April 2005

*Affiliated with University of Kansas at the time of research

PREFACE

The Kansas Department of Transportation's (KDOT) Kansas Transportation Research and New-Developments (K-TRAN) Research Program funded this research project. It is an ongoing, cooperative and comprehensive research program addressing transportation needs of the state of Kansas utilizing academic and research resources from KDOT, Kansas State University and the University of Kansas. Transportation professionals in KDOT and the universities jointly develop the projects included in the research program.

NOTICE

The authors and the state of Kansas do not endorse products or manufacturers. Trade and manufacturers names appear herein solely because they are considered essential to the object of this report.

This information is available in alternative accessible formats. To obtain an alternative format, contact the Office of Transportation Information, Kansas Department of Transportation, 700 SW Harrison, Topeka, Kansas 66603-3754 or phone (785) 296-3585 (Voice) (TDD).

DISCLAIMER

The contents of this report reflect the views of the authors who are responsible for the facts and accuracy of the data presented herein. The contents do not necessarily reflect the views or the policies of the state of Kansas. This report does not constitute a standard, specification or regulation.

ABSTRACT

This paper discusses results from an analytical study concerning the long-term evaluation of two fiber-reinforced polymer composite bridges in Kansas. A background on current non-destructive evaluation methodologies for monitoring structural systems and typical sensors that are used with non-destructive evaluation techniques is discussed. The results of the finite element models of the bridges are presented. A procedure for selecting and installing appropriate systems for non-destructive evaluation of the fiber-reinforced polymer composite bridges is described.

The purpose of this paper is to address specific questions proposed by the Kansas Department of Transportation regarding the performance of fiber-reinforced polymer composite decks installed in the fall of 1999 on two existing bridges, and to identify possible long-term performance problems. The main objectives are:

- To determine if composite action develops between the fiber-reinforced polymer composite deck, saddle and steel girder. And if composite action does develop, estimate the improved capacity of the bridge.
- To determine if vibration of the bridge may lead to structural deterioration.
- To evaluate the effectiveness of the bolted connections.

The data collected from the non-destructive testing on the bridge suggests that composite action may not exist. The dissipation of energy recorded using accelerometers demonstrates that the fiber-reinforced polymer composite deck and steel girder behave independently. However, studies using finite element analyses show that composite action can develop if bonded. There is excessive vibration within the fiber-reinforced polymer deck. The results of non-destructive testing performed on one bridge showed that the deck dissipates energy in a wide

frequency range. This type of energy dissipation is typically a result of excessive vibration and excitation. This is a concern and further investigation is recommended.

From the finite element analyses, the stress levels under normal traffic loading are not a concern. However, the combination of loads due to thermal differential and induced vibration due to heavy trucks, can produce large stresses within the bolted connections that may lead to material fatigue.

TABLE OF CONTENTS

LIST OF FIGURES

LIST OF TABLES

Chapter 1

Introduction

1.1 Background

Throughout Kansas, there are many aging civil structures in need of rehabilitation. The structures have often become too deteriorated for their intended use and require some major repairs so that they can be serviceable again. The Kansas Department of Transportation (KDOT) is utilizing fiber-reinforced polymer (FRP) composites to retrofit and replace certain deteriorating metal and concrete bridge decks. The KDOT believes that using FRP composites to rehabilitate deteriorating bridges will be economically feasible for certain bridges. The bridges that the KDOT has targeted to implement FRP bridge decks are single span bridges found in rural areas that have been in service for more than thirty years. They consist of steel girders and a concrete and metal deck that has deteriorated. In most cases, the steel girders are still serviceable. However, the concrete and metal deck have deteriorated and require replacement. Two existing bridges located in Crawford County, Kansas have already had the deck replaced with FRP composites and are the main focus of this research. Because the two existing bridges are identical, only one bridge was analyzed for this project.

1.2 Description of the Bridge

The two-lane bridge spans approximately 13.7 meters over a riverbed in southern Kansas (Figures 1.1, 1.2 and 1.3). The bridge consists of fourteen W21x68 steel girders that are embedded approximately 343 mm into the abutments (Figure 1.4). The new FRP composites that replace the existing metal and concrete deck consist of FRP composite saddles that straddle the top flange of the existing W21x68, and FRP honeycomb deck panels, which lie on top of the

FRP composite saddles. The FRP composite saddle and deck panel attach to the existing steel girder by a clamping device designed by KDOT (Figure 1.5). The clamping device consists of structural FRP pultruded shapes, steel plates and high strength bolts and is installed on both sides of the FRP saddle. The clamps are installed at every panel joint and on every third girder (Figure 1.3). Chapter 3 discusses the clamp and physical properties of the FRP composites in detail.

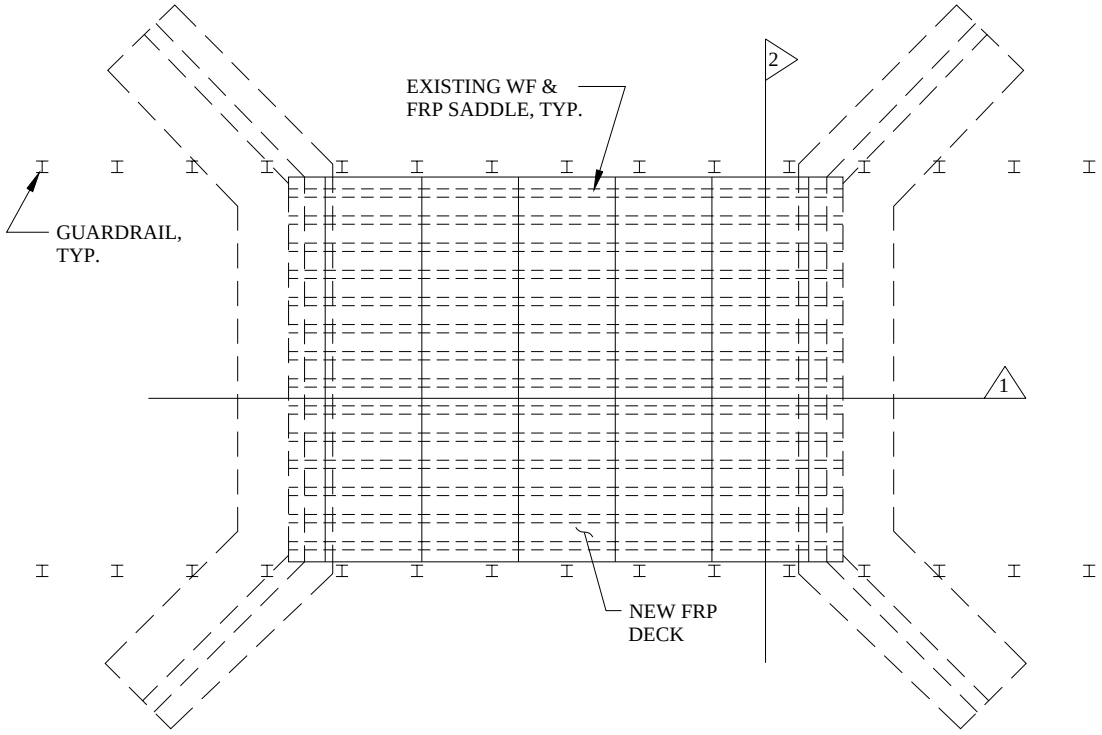

Figure 1.1 – Plan of the FRP Composite Bridge
(Provided by KDOT)

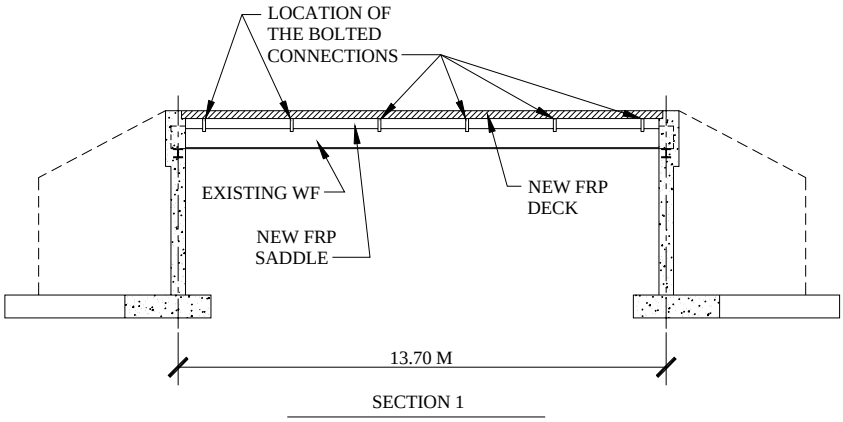

Figure 1.2 – Section 1 of the FRP Composite Bridge
(Provided by KDOT)

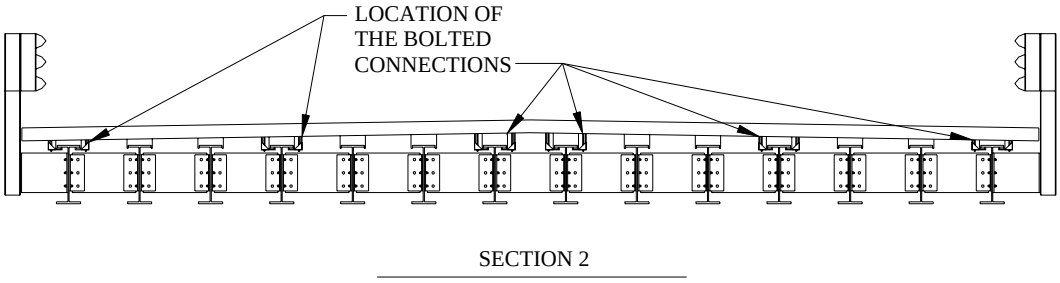

Figure 1.3 – Section 2 of the FRP Composite Bridge
Describing the Location of the Bolted Connection

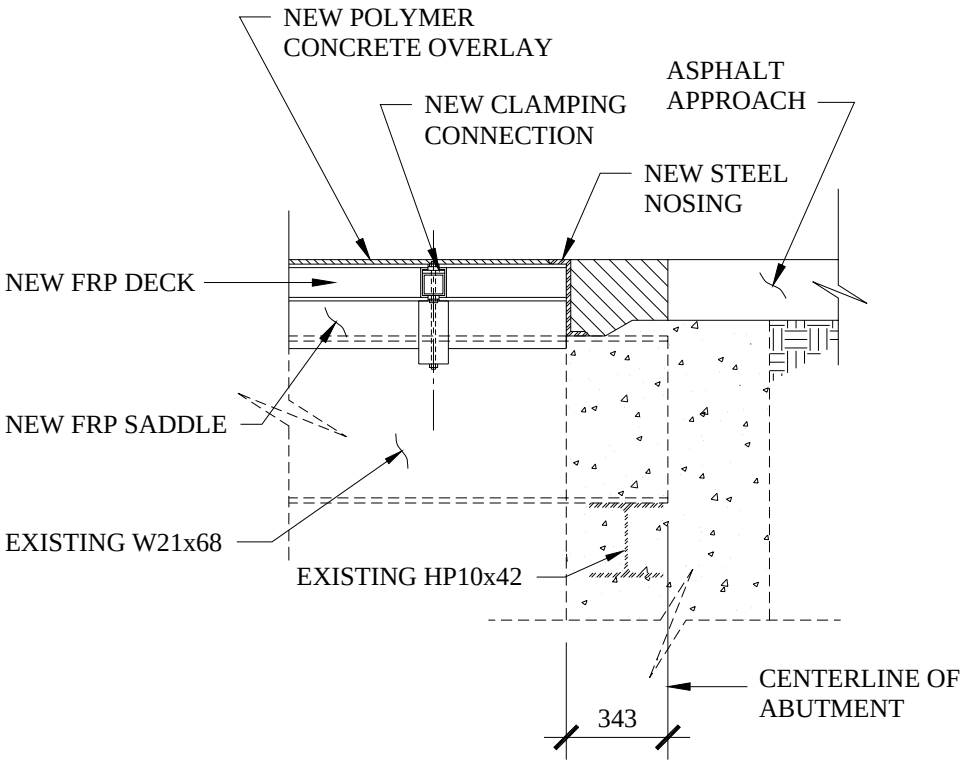

Figure 1.4 - Detail of Embedded Girder into the Abutment

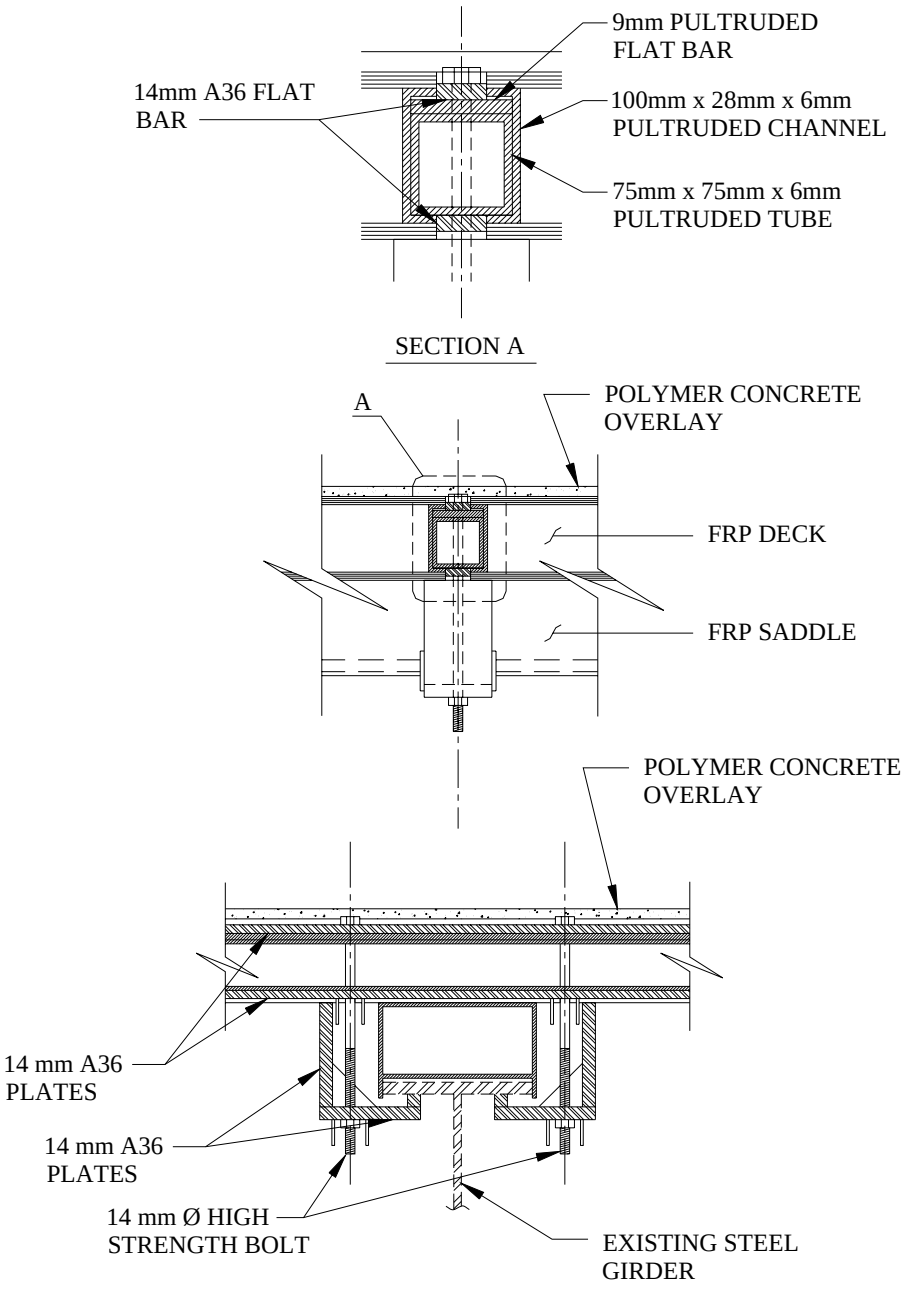

Figure 1.5 - Details of the Clamping Device Invented by KDOT

1.3 Objective of the Project

There are two primary objectives for the project:

1. Provide a long-term behavior assessment of the FRP composites of the bridges in Crawford County, Kansas.

2. 2.Select a feasible non-destructive method to monitor the long-term behavior of the bridges.

To accomplish the objectives, non-destructive testing was performed on the bridge as well as finite element analyses of the modeled bridge. An assessment of the long-term behavior and a feasible monitoring plan were determined from the analyses using a suite of loading cases including temperature differential, vibration, and traffic loading conditions.

The first part of the project, described in Chapter 2, was to conduct a literature search on available non-destructive evaluation methods, structural health monitoring techniques, and typical sensors used to monitor civil structures. The second part of this project was to construct finite element models to predict the behavior of the bridge, which are described in Chapter 3. Chapter 4 discusses the analyses of the finite element models, and the results are provided in Chapter 5. Finally, Chapter 6 provides an implementation plan for selection and location of appropriate monitoring devices.

Chapter 2

Structural Monitoring and Sensor Technologies

2.1 Introduction

This chapter discusses in detail two types of structural monitoring techniques, a description of the available sensors that can be used in structural monitoring and the advantages and disadvantages of each technique for evaluation of the KDOT FRP composite bridges for long-term behavior assessment.

2.2 Structural Monitoring Techniques

Two structural monitoring techniques for possible implementation on the FRP composite bridge are:

- Non-destructive evaluation (NDE).
- Structural health monitoring (SHM).

Because the KDOT FRP composite bridge employs innovative materials that have not been previously tested for long-term behavior in these conditions, it is important to understand the benefits of each monitoring technique to select an appropriate monitoring technique.
NDE and SHM have many similarities. Both methods can be used to detect damage and serviceability of the FRP composite bridge, help locate where damage has occurred and the severity of the damage, and can target specific materials or structural elements within the bridge. Both monitoring techniques can incorporate a number of different sensors to acquire the desirable measurements. In addition, the systems use similar devices to gather the measurements from the sensors.

There are a few differences between the structural monitoring techniques. SHM integrates the sensors and devices into the structural system so that the structure can be continuously monitored. The sensors can be embedded, attached internally, or attached externally. Monitoring equipment can be housed in a mechanical box near the site to gather data and transmit information off the site. NDE usually requires that the equipment be transported and operated on site.

2.2.1 Non-Destructive Evaluation

Non-destructive evaluation, NDE, (also known as non-destructive testing or NDT) is a descriptive term used for the examination of materials and components without changing or destroying their usefulness (NDTA, 1996). NDE plays a crucial role in many facets of engineering work and is necessary to assure safety and reliability. Typical examples of its application are for aircraft, motor vehicles, pipelines, bridges, buildings, trains, power stations, refineries and oil platforms. Materials, products and equipment which fail to achieve their design requirements or projected life due to undetected defects may require expensive repair or early replacement. Such defects also may be the cause of unsafe conditions or catastrophic failure, as well as loss of revenue due to unplanned shutdown. Non-destructive testing can be applied to each stage of construction for large civil engineering applications. Materials, welds, and connections can be examined using NDE and either accepted, rejected or repaired. NDE techniques can then be used to monitor the integrity of the item or structure throughout its design life. NDE is a quality assurance management tool, which can give impressive results. Effective use requires an understanding of the various methods available, their capabilities and limitations, and knowledge of the relevant standards and specifications for performing the tests.

All current NDE methods can be classified into one of four levels according to their performance (Sikorsky, 1999):

Level I – methods that only identify if damage has occurred.

Level II – methods that identify if damage has occurred and simultaneously determine the location of damage.

Level III – methods that identify if damage has occurred and determine the location of damage as well as estimate the severity of the damage.

Level IV – methods that identify if damage has occurred, determine the location of damage, estimate the severity of damage, and evaluate the impact of damage on the structure.

Typically, a NDE system consists of three components (Figure 2.1): 1) a network of sensors for collecting sensor measurements, 2) data acquisition equipment for gathering all of the sensor measurements, and 3) software to interpret the sensor measurements to real physical data. Depending on the input data, these techniques can be divided into two types of systems: 1) passive sensing systems without known input (with sensors only) and 2) active sensing systems with known input (with both sensors and transducers, or actuators).

2.2.1.1 Passive Sensing Diagnostics

For a passive sensing system, only sensors are installed on the structures. While the structures are in service, sensor measurements are collected, and software converts the measurements into real physical data. In this case, the loading is not controlled and is unknown. This data is then compared to a set of reference data, which can be theoretical or based on data from a controlled test previously performed. From this comparison, estimates of the condition of the structures can be obtained. Hence, the techniques of data comparison for interpretation of structural conditions are crucial for a reliable system.

Because the energy input into the structure is typically random and unknown, the corresponding sensor measurements reflect the response of the structures to the unknown input energy, or loading. This type of diagnostics is primarily used to determine the unknown input energy, such as external loads, temperature, pressure, etc. (Chang, 1999).

2.2.1.2 Active Sensing Diagnostics

For an active sensing system, known external mechanical or non-mechanical loads are applied to the structure through devices that have been temporarily attached such as transducers or actuators, or other loading predetermined. Because the input energy, or load, is known, the difference in the local sensor measurements is strongly related to a physical change in the structural condition, such as the introduction of damage.

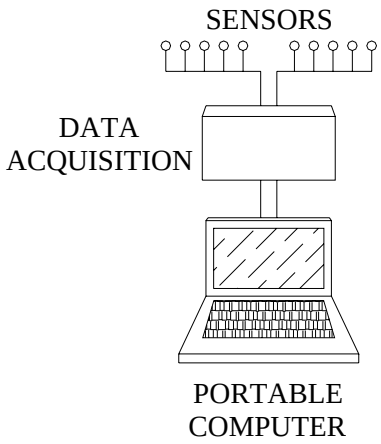

Figure 2.1 - Schematic Diagram of Non-Destructive Evaluation

Combining a passive sensing diagnostic and an active sensing diagnostic can be beneficial. The structure could be monitored using an active sensing system to determine the response from a known input energy, or load, such as deflection, stiffness, vibration, etc. The structure could then be monitored using a passive system to determine the response from

unknown input energy, such as deflection, stiffness, vibration, etc, caused from traffic induced loads, thermal differential, etc. The measurements from the active sensing diagnostic and passive sensing diagnostic systems can be compared to help predict the unknown input energy on the structure. Once the unknown input energy is determined, better predictions can be made on the future condition of the structure.

2.2.1.3 Advantages and Disadvantages of NDE

One advantage of NDE is that it can examine the materials and components of a structure without changing or destroying their properties. Depending on the complexity of the structural system, NDE is simple and produces good results in a short amount of time. NDE is better suited for smaller, simple structural systems, so that larger expensive equipment is not needed to assist in installing the sensors and devices. The two KDOT FRP composite bridges are good examples of such structures.

A disadvantage of NDE can be found when applied to complex systems. The amount of labor and time required to properly install the network of sensors for NDE is proportional to the complexity of the structural system. In addition to expensive labor, extra equipment may be required to install the sensors, which will increase the overall cost. Another possible disadvantage in using NDE is that the structure may need to be shutdown temporarily during the evaluation and installation.

2.2.2 Structural Health Monitoring

Structural Health Monitoring, SHM, is similar to NDE in that it examines materials and components without changing or destroying their usefulness. However, structural health monitoring is a system that continuously monitors, inspects, and detects damage of structures with the least amount of labor possible (Chang, 1999). To achieve this, the sensors and sensing

equipment are embedded or permanently attached to the structure, and are networked together to collect data without interruption. Continuously monitoring the structural conditions makes it possible to report the conditions of the structure through a local network or to a remote center automatically. Therefore, the primary difference between NDE and structural health monitoring is that SHM consists of a built-in diagnostic system.

The primary components of SHM are similar to the components for NDE methods such as: a network of sensors for collecting sensor measurements, data acquisition equipment for gathering all of the sensor measurements, and software to interpret the sensor measurements to physical data. However, SHM incorporates a local network or remote center to send information (Figure 2.2). Furthermore, depending on the input energy, these techniques also can be divided into two types: passive sensing systems and active sensing systems.

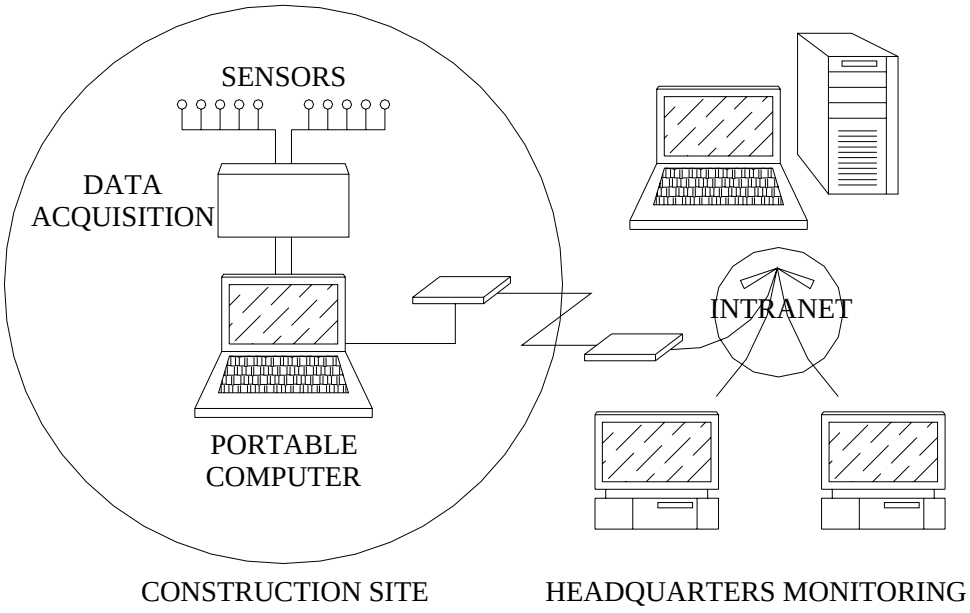

Figure 2.2 - Schematic Diagram of Structural Health Monitoring

2.2.2.1 Passive Sensing Diagnostics

The SHM procedure is similar to that of the NDE, the primary difference being that the sensors are permanently installed on the structure for SHM, so that the sensor measurements are recorded continuously while the structure is in service. These measurements are then compared with an existing set of data to determine the health of the bridge. The SHM system requires either a database, which has a history of pre-stored data, or structural simulations that could generate the needed reference data.

2.2.2.2 Active Sensing Diagnostics

The active sensing diagnostic procedure of SHM is similar to that of the NDE. Again, the primary difference is that the measurements from the permanently attached sensor are continuously recorded.

2.2.2.3 Advantages and Disadvantages of SHM

Many benefits can be obtained using built-in systems of networks. Real-time monitoring and reporting will save in maintenance costs. Having minimal human involvement will reduce labor costs, downtime, and human error. Having system automation will improve the safety and reliability of the structure, because damage can be detected in real time and repaired with minimal downtime. With the reduced downtime and improved reliability, in-service structures could be used more productively with less cost by benefiting from the safe operation of the structures. Knowing the condition of the structure will increase the reliability of the structure and result in a more economical system because damage can be repaired early once it has been detected, thereby minimizing the threat of severe damage and costly repairs.

The primary disadvantage of using SHM is the upfront cost and planning. SHM expenses become part of the construction costs rather than post-construction as does NDE.

2.3 Sensors

Sensors can play an important role in the longevity of a structural system. The combination of advanced sensors and monitoring devices can create a reliable method to monitor the performance of the structure. There are multitudes of different sensors that have applications for several different industries. Sensors can be used alone, in a series or a network. As a simple description, sensors convert information about the environment such as temperature, force, pressure, etc., into an electrical signal. Table 2.1 lists several available sensors and their applications that would be used to monitor structural systems.

Table 2.1 – Sensors and Their Applications

Sensor	Application
Fiber Optics	Applications ranging from civil infrastructures to aircraft structures
Fiber Bragg Grating Strain Sensors	A type of fiber optic sensor used in monitoring long span bridges
Piezoelectric Transducers	Used as both sensors for measurements and actuators for generating diagnostic signals for monitoring damage in structures made of both metal and composites
Strain Gages	Used for the damage assessment of bridges, buildings, and many other systems
Acoustic Emission	Used in aerospace and civil industries to measure composite matrix delamination and crack growth in composites and metal structures
Accelerometers	Used in several industries to measure frequencies for modal and other analyses
Linear Variable Displacement Transducers	Used to measure displacement in structural elements

2.3.1 Sensor Implementation

Although there are a plethora of sensors available in the market, some sensors may be more applicable than others. Depending on the measurements needed and the scale of the

structure, a network of reliable and economical sensors may be required. The following are key technology issues to consider in sensing:

- **Distributed sensors:** Techniques will need to be developed to distribute a large array of sensors in a network that is economical. This area is of particular importance for civil structures because of their size.
- **Remote sensing:** Wireless communication between local sensors and a controller may be needed. As the number of sensors increase with the size of the structure, so does the number of communication wires. The management and handling of multiple wires can be difficult and challenging. With remote sensing capability, data can be gathered locally and the structure can be monitored remotely.
- **Sensor reliability and integrity:** Failure of sensors or actuators may result in faulty signals or cause the systems to become unreliable. The integrity of sensors and actuators under various loading conditions and environments for particular applications should be studied before implementation. The long-term behavior of sensors and actuators and the interfacial strength between the sensors/actuators and the host structures also need to be considered.

2.3.2 Diagnostic Signal Generation

Once there is a basic understanding of the different types of monitoring techniques and the key issues regarding the selection of the sensors are considered, it is important to understand how sensors work.

For passive sensing systems, sensors measure the response of the structure to an unknown external thermal or mechanical load, which must then be determined for a reliable analysis. For active sensing systems, additional signals are measured by the sensors in response to known excitation generated by actuators or transducers in a controlled environment. These controlled diagnostic signals are used to excite the sensor measurements so that any local abnormal

behavior in the structure can be identified. Accordingly, the determination and generation of the diagnostic signals will critically affect the measurements and the identification.

2.3.3 Signal Processing

In the data collection process, an enormous amount of data can be obtained that are irrelevant to the interest of the particular concern. In addition, the data can be corrupted by the environment and noise, and create problems interpreting the data. The data should be filtered, using algorithms or other means that have been developed for the proposed application, to assure that the data generated was from the appropriate external force. It is important to filter all of the information generated by the sensors so that the desirable data can be obtained.

2.3.4 Damage Interpretation/Identification Analysis

The damage detection/identification analysis plays a major role in the monitoring system and can be regarded as the "brain" of the system. The accuracy and reliability of the system strongly relies upon the accuracy and reliability of the analysis for relating the sensor measurements to the physical changes in the structures. Damage or an abnormal condition may not occur at the location where the sensor is located. Therefore, sensor information should be extrapolated to predict damage that occurs at a distance away from the location of the sensor. It is beneficial to estimate probable locations of future problems to determine the best location for the sensor.

Determination of the physical condition of a structure based on sensor measurements is a nonlinear inverse problem. Several numerical and analytical techniques have been developed for the proposed applications. Some promising methods include modal analyses, system identification, neural network algorithms, generic algorithms, and optimization algorithms. However, most results are limited to controlled laboratory environments and on simple structural

configurations. In practice, most techniques require an extensive history of data of the structure in both undamaged and damage conditions.

2.3.5 Description of the Sensors

It is important to know what each sensor can measure, and understand the advantages and disadvantages of each sensor to determine the sensor that will provide the most desirable measurement. The user must be familiar with the specific equipment needed to use the sensor and the relative costs of installation. A good understanding is also required on how the sensor measurements are generated so that an appropriate identification method can be chosen to interpret the measurements.

2.3.5.1 Fiber Optics

Fiber optic sensors can be used to measure many different properties in several types of materials. Fiber optic sensors can be embedded in a structural material such as concrete or FRP composites or bonded to the exterior of the structural element. Essentially, fiber optic sensors can be used in three different ways (Measures et al, 1991):

1. Those that can be damage sensitized so that they fracture when the material is critically loaded.
2. Those that can be made into very sensitive strain sensors that can detect acoustic energy released when the material is subjected to sufficient load to cause internal damage.
3. Those that can be combined with devices so that the device can produce a warning signal when a specified intensity is reached.

These three different methods can be classified into two ways:

- Those that use the optical fiber itself as the sensing medium.

- Those where the fiber acts as a light guide to connect the light to a sensor cell and returns the light from the sensor cell to an analyzing system which may be spectroscopic or electronic.

Fiber optic sensors can be used to monitor such parameters as temperature, pressure, viscosity, residual strain, and degree of cure based on fluorescence of the resin in the composite (Udd, 1996). They also may be used to measure acoustic signatures, changes in strain profiles, delamination of composites, and other indications of changes in structural characteristics of fabricated parts.

There are three basic devices needed to use fiber optic sensors: a light emitting device (LED) which is the source light to be sent down the glass fiber, a data acquisition device to collect all of the sensor measurements, and a processing unit for interpreting the measurements. The fundamental make-up of the sensor (an optical fiber strain gage – Figure 2.3) consists of an input/output fiber and a reflector fiber separated by an air gap and gage length. The source light travels through the glass fiber and is reflected off the reflector fiber and is returned back to the source where it is converted to an electric signal and processed.

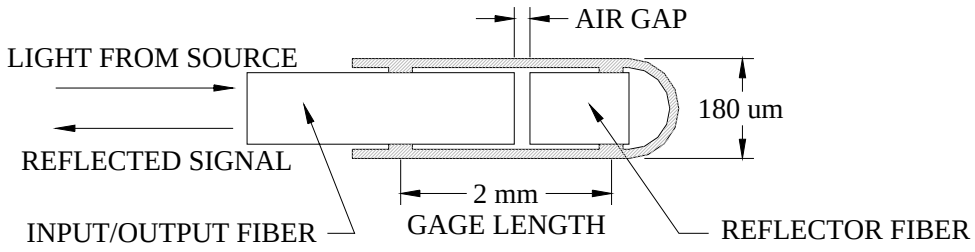

Figure 2.3 - Schematic Diagram of the Sensing Part of an Optical Fiber Sensor

Damage sensitized sensors fracture when the stresses in the host structure reach a predetermined threshold. In the case of the sensor being embedded in a composite structure, the

fiber will fracture when the host structure delaminates and causes a disruption in its transmitted light. This use of the sensor in composites is more sensitive to the core of the delamination rather than the edge. Fiber optics can be used to detect acoustic emissions by incorporating Michelson interfermetric fibers that detect the energy released when a the matrix of the composite cracks, which could prove useful in determining internal damage if embedment is not possible such as with the KDOT fiber composite bridge. Also, the sensors can be embedded in or attached to the structural components during the manufacturing process so that the structural components of a large structure, which may be impractical to reach and install after construction, can be monitored. Unlike health and damage assessment systems, which simply monitor changes in the structure, these control systems measure the environmental effects acting on the structure, as well as, the impact those environmental effects have on the structure.

- **Advantages**: Fiber optic sensors have a series of important advantages over conventional electronic sensors. They are small, often made with an overall diameter of 125μm or less resulting in a hair-like sensor that can be embedded in many types of composites without changing the mechanical properties. Fiber optic sensors can be made environmentally rugged and able to withstand the temperatures and pressures associated with the manufacture of FRP composites. Another advantage of fiber optic sensors is that they have electromagnetic immunity. They are lightweight, small in size, have low transmission loss, and are corrosion resistance. They also may be used to provide new capabilities for monitoring very large structures, and can be combined with telecommunications to carry the information long distances.
- **Disadvantages**: Some of the limitations associated with fiber optic sensors demonstrated by damage-sensitized sensors, because once they fracture, they must be replaced. In certain areas where the sensor is not accessible, i.e. the underside of a long span bridge, the sensors might not

be replaceable. Also, determining residual strains and delamination are not possible for existing structures because these sensors must be embedded and pre-installed.

2.3.5.2 Fiber Bragg Grating Strain Sensing

FBG are produced by focusing ultraviolet light on a small section of optical fiber at a prescribed incident angle. This process induces a modulation in the local index of refraction such that the grating acts as a narrow-band optical filter, with light being reflected backwards at a wavelength dependent on the grating spacing which is determined, in part, by the original incident angle of applied ultraviolet light. This "tunable" wavelength encoding allows for easy multiplexing of many Fiber Bragg gratings on a single optical fiber strand. Each FBG can be manufactured to reflect light at a unique initial wavelength, corresponding to a unique location on the structure, and any reflected wavelength shift can be attributed to strain at the location. Fiber Bragg gratings, FBG, are emerging as important elements for both the optical fiber communications and sensing fields. Applications include use in a wide range of devices for wavelength routing, filtering, gain flattening, and dispersion compensation in communications systems, and a range of distributed strain and temperature sensing systems. These sensors also can be used to monitor long-term vibrational responses, and determine real time deflections, as well as acceleration.

Fiber Bragg gratings represent a relatively simple, compact, and low-cost approach to measuring strain or temperature for many applications (Todd et all, 1998). The simplicity arises because there is no need to measure the optical phase, hence no need for a coherent light source. Light demodulation instruments are difficult and costly to manufacture, thus using FBG results in a significant cost savings. Because FBG can be written at different wavelengths, many individual sensors can be wavelength-division-multiplexed and integrated onto a single fiber

optic strand. FBG may be fabricated on most commercially available fibers. The reflection and transmission response from the gratings also can be custom designed to a given specification. The Fiber Bragg gratings can be bounded on many surfaces using an adhesive.

A FBG strain measurement system utilizes four diodes as optical sources, six couplers, two fiber optic filters, two photodetectors, electronic parts, and a laptop computer. The light emitted by the diodes are reflected back from the sensor array and focused through the filters, which pass only a very narrow band wavelength that is dependent upon the spacing between mirrors in the device. Applying a rapidly stepped voltage to drive the mirrors controls this spacing. The passed light signal is sent through a photodetector and differentiated. The zero crossing of the differentiated signal corresponds to the peak wavelengths of the reflected light. This correlation between the ramp voltage level and shifts in the zero crossing rate can be used to determine the strain for each sensor, because wavelength shifts are proportional to strain in the grating.

- **Advantages**: Because a FBG sensor is a form of a fiber optic sensor, FBG sensors have similar advantages to that of fiber optics. However, the advantage of using FBG sensors over fiber optics is being able to link several sensors together in a series or network. The use of FBG sensors also requires less expensive equipment.
- **Disadvantages**: The disadvantages are similar to that of fiber optic sensors.

2.3.5.3 Piezoelectric Transducers

Piezoelectric materials are used as both sensors for measurements and actuators for generating diagnostic signals for monitoring damage in structures made of metal and composites. Depending on the material of the crystal, it can be used to detect several

measurements such as pressure, deformation, or temperature. For example, the quartz crystal can detect deformation.

Typically, piezoelectric transducers consist of one or more crystals stacked between appropriate insulators, connectors, and load distribution plates (Figure 2.4). The different crystals used are quartz, lead zirconite, barium titanate, or tourmaline. An electrical signal is generated by a charge that appears across the faces of the crystal when it is deformed by the force applied. This electrical signal is then converted to desired results, using a processor, i.e. laptop computer.

The piezoelectric crystal has a high output level. Under a force of 13500 Newtons, a quartz crystal 12.7 millimeters in diameter and 1.59 millimeters thick will produce an output of 3000 mV across a 0.1 microfarad capacitor (Moore, 1976). This output, however, must be operated with a very high impedance read-out device.

- **Advantages**: The advantages of piezoelectric transducers are low leakage, the ability to measure slow varying pressures, low frequency variations, the ability to operate at higher temperatures, and shock resistance (Moore, 1976). The cost and ease of use are attractive as well. These sensors are easy to apply and obtain results without a disruption of service.
- **Disadvantages**: A disadvantage of sensors made of piezoelectric materials is that the poor signal to noise ratio can affect the accuracy of the results.

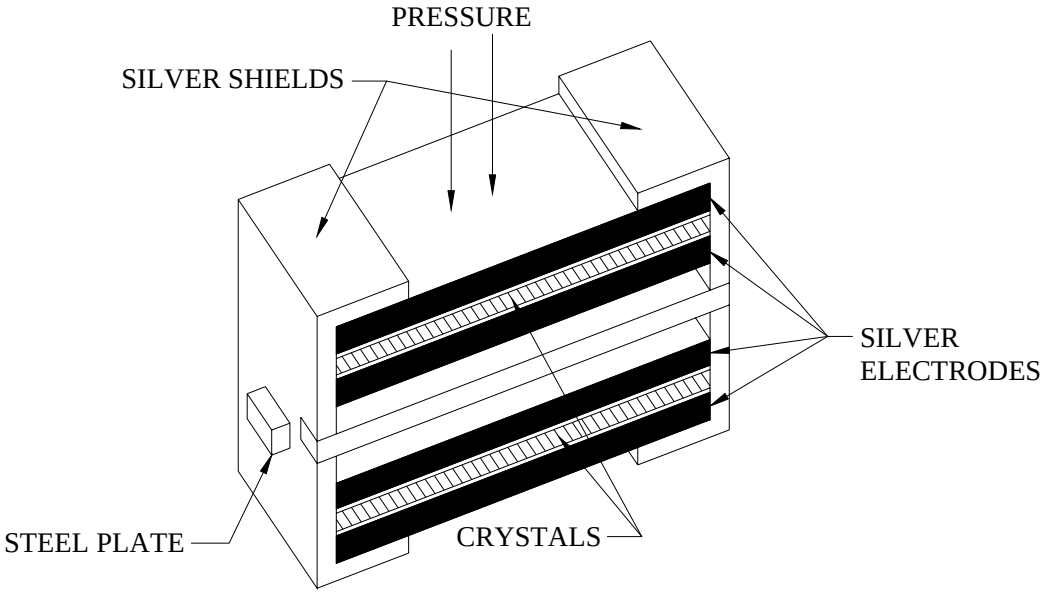

Figure 2.4 - Schematic Diagram of a Piezoelectric Transducer

2.3.5.4 Strain Gages

Strain gages are transducers that provide an indirect measurement of force by measuring the deformation of an object under the influence of an external force (Moore, 1976). The gages measure the small displacements, or strains, associated with the stress on solid objects, such as the bending stresses in a beam. Strain gages are variable resistors, constructed in such a way that their resistance varies in proportion to the strain present on the surface of the material to which the gages are bonded. Depending on the direction of the force applied to the material, the change in resistance can be positive or negative.

All electrical components exhibit some resistance to the flow of electricity, which can be measured by electronic instrumentation (Moore, 1976). The strain gage is a strain-sensitive component bonded to the surface of the test specimen to measure strain. When the strain gage is elongated, its resistance changes in direct proportion to the strain. The strain can be determined by measuring the change in electrical resistance. A voltage is sent across a Wheatstone bridge

with a known resistance. When the load or force is applied the resistance of the strain gage (wire) will cause the output voltage to change. This electrical signal (output voltage) can be converted to useful information via a processing unit, i.e. computer.

The most variable part of a strain gage transducer is the wire material (Moore, 1976). The resistivity of different materials that can be used for wires can change the results. Some reliable wires are made of manganese and gold alloys, and are available in easily installed cells that are isolated by a flexible thimble and filled with a non-conducting fluid.

Strain gages are applied by either bonded or unbonded techniques (Figure 2.5). The unbonded installation offers high sensitivity and moderate accuracy (Moore, 1976). Bonded strain gages suffer less from long-term instability, but are only half as sensitive as the unbonded. In strain gage transducers, a wire, foil, or semiconductor resistor element usually is bonded to a diaphragm. The deflection of the diaphragm alters the gage resistance and unbalances an associated bridge.

- **Advantages**: The advantages with strain gage elements are that they work well for dynamic measurements, offer fast response, low source impedance and minimum mechanical motion (Moore, 1976). The gages also are small with little weight. These sensors are easy to apply and provide reliable results without extended disruption of service to the structure.
- **Disadvantages**: Some of the disadvantages include a loss of accuracy in use due to hysteresis, and rather costly output measurement devices (Moore, 1976). Short-term total accuracy is 1% of the theoretical value. However, creep and hysteresis make frequent recalibration necessary. Further, zero tends to shift because of long term changes in wire resistivity and stress relief.

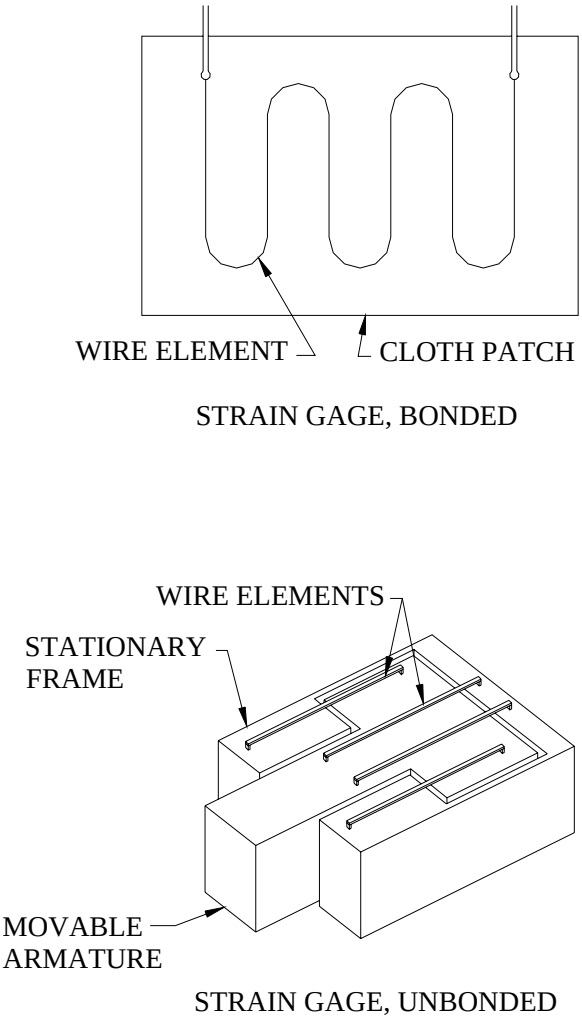

Figure 2.5 - Schematic Diagram of a Bonded and Unbonded Strain Gage

2.3.5.5 Acoustic Emission

Acoustic emission monitoring (AE) involves listening to the sounds made by a material, structure or machine under load, which are usually inaudible to the human ear, and drawing conclusions about what is heard (NDTA, 1996). An acoustic emission is a sound wave or a stress wave that travels through a material as the result of a sudden release of strain energy (Figure 2.6). The operator can "hear" the sound of a crack as it propagates and is arrested. For

example, the sound associated with the plastic deformation that takes place at the tip of the crack can be detected before propagation.

The technique involves attaching one or more ultrasonic microphones to the object and analyzing the sounds using computer-based instruments. The noises may arise from friction, crack growth, turbulence (including leakage) and material changes such as corrosion. Applications include testing pipelines and storage tanks (above and below the ground), fiberglass structures, rotating machinery, weld monitoring and biological and chemical changes.

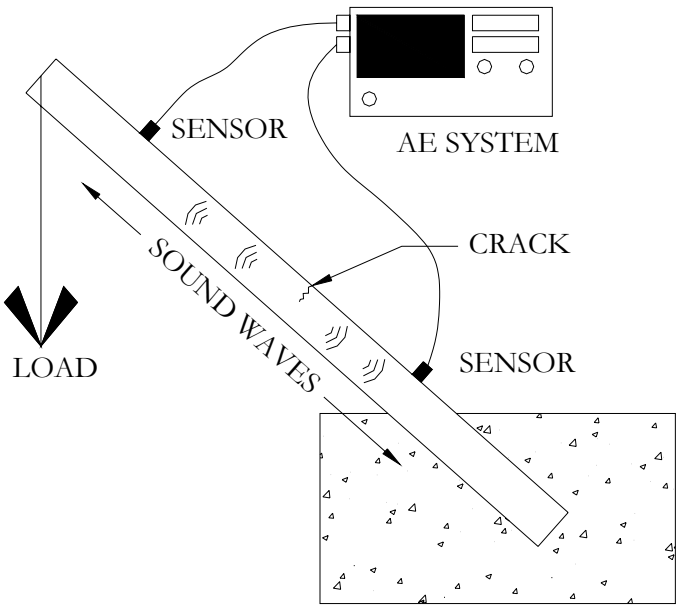

Figure 2.6 - Schematic Diagram of Acoustic Emission

- **Advantages**: The advantages of AE are that entire structural systems can be monitored from a few locations, the structure can be tested in use without disrupting service and continuous monitoring with alarms is possible. Microscopic changes can be detected if sufficient energy is released and source location also is possible using multiple sensors. Another advantage of acoustic monitoring is that it has the capability of detecting crack growth in real time. In fact, AE only responds to active flaws. This unique feature of AE makes it a

prime candidate for crack characterization in highway bridges. The sensors also are easy to apply and provide reliable results without extended disruption of service to the structure.

- **Disadvantages**: Some disadvantages with AE sensors are that the location of the sensor must not coincide with the location of any bolts that might exist on a structure. The acoustic emissions from the bolts during loading may affect the results.

2.3.5.6 Micro-sensors and MEMS

Microsensors and Microelectromechanical Systems (MEMS) are currently being applied to the structural health monitoring of critical structural components (Varadan et al., 1999). This approach integrates acoustic emission, strain gauges, accelerometers and vibration monitoring devices with signal processing electronics to provide real-time indicators of structural failure.

Microsensors are basically silicon, piezoelectric wager or polymer devices that convert a mechanical signal into an electronic signal with the aid of microelectronics technology (Varadan et al., 1999). In smart structures, the electronic signal obtained from the sensors is amplified and fed to Application Specific Integrated Circuit (ASIC) chips. Using the intelligence in the electronics, the signal will be processed by the microprocessor and controller and then fed to the actuator. Using this type of integrated or smart sensor, one could achieve many actuation functions locally or remotely at several locations using wireless telemetry devices.

One set of microsensors being developed for health monitoring and condition-based maintenance is based on generating Lamb, Love, Bulk or Rayleigh surface waves in structures (Varadan et al., 1999). Lamb waves are useful for sensing impact damage, cracks, delamination, 'kissing bonds' and corrosion. Love waves are ideal for detecting ice formation, and acoustic emission signals for monitoring the onset of crack formation and propagation. Bulk waves are

useful for propagating both longitudinal and shear waves into structures. Rayleigh surface waves are used for sensing deflection, strain, temperature, humidity, pressure, and acceleration. These waves can be generated by Inter Digital Transducers (IDT) which are either micromachined, etched or printed on special cut piezoelectric wafers or on certain piezoelectric film deposited on silicon using the standard microelectronics fabrication techniques, and integrated with MEMS (Figure 2.7).

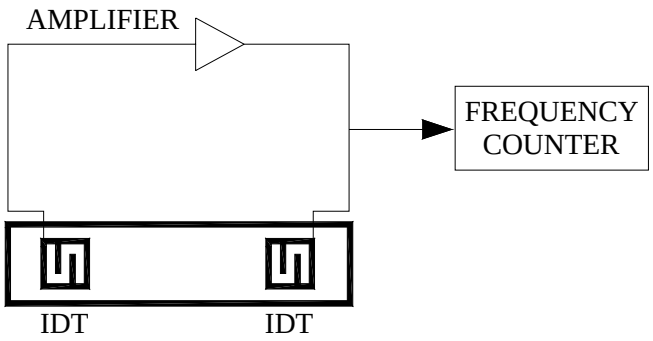

Figure 2.7 - Schematic Diagram of a Typical IDT Oscillator Sensor

The MEMS-IDT sensor is based on the fact that the waves traveling time between the IDTs change with the variation of physical variables (Varadan et al., 1999). One of these IDTs acts as the device input and converts signal voltage variations into mechanical waves of the types mentioned above based on the piezoelectric crystal cut. The other IDT is employed as an output receiver to convert the mechanical waves into output voltages. These devices are reciprocal in nature; as a result signal voltages can be applied to either IDT with the same end result. To obtain high sensitivity, MEMS-IDT sensors are usually constructed as electric oscillators using the IDT device as frequency control components. By accurately measuring the oscillation frequency, a small change of the physical variables can be detected by the sensors.

An amplifier connects two IDTs on a piezoelectric wafer so that oscillations result because of the feedback of the waves propagating from one IDT to the other (Varadan et al., 1999). The oscillator includes an amplifier and requires electrical power supply and cannot be wireless. The operating frequency range of such devices is from 10 MHz to a 2-3 GHz, which directly matches the frequency range of radios and radars. When an IDT is directly connected to an antenna, the waves can be excited remotely by electromagnetic waves.

For remote wireless sensing, the receiving IDT can be replaced by a set of reflectors (Varadan et al., 1999). The reflectors can be programmed such that each sensor will have its own 'bar code' for identification. This kind of sensor identification is particularly attractive when many microsensors are used at various locations on the structure. These sensors can be surface mounted or mounted inside a composite material during the fabrication process to advance the state-of-the-art of smart structure application and design for future bridges.

- **Advantages**: The advantage of using MEMS sensors are that they offer a much wider dynamic range and better linearity than most sensors. Because of the small size of each sensor, MEMS sensors can be placed anywhere on the structure in addition to transmitting measurements with or without wires.
- **Disadvantages**: The disadvantage of using MEMS sensors is the high cost of the micro-sensors, equipment, system integration, and complexity.

2.3.5.7 Accelerometers

Accelerometers are used to determine base-line vibration signatures in modal testing to extract certain modal parameters such as frequencies of mode shapes. This measurement can be further implemented for a bridge monitoring system to indicate the condition, damage, or remaining capacity of the structure.

A conventional accelerometer consists of a proof mass, a spring, and a position detector (Figure 2.8). Under steady-state conditions, the proof mass that experiences a constant acceleration will move from its rest position to a new position, which is determined by the balance between its mass times the acceleration and the restoring force of the spring (Soloman, 1999). Using a simple mechanical spring, the acceleration will be directly proportional to the distance traversed by the proof mass from its equilibrium position.

- **Advantages**: Modal testing has certain advantages. It is easy to use and can be cost effective. The sensors, measurement systems, signal processing instruments and software has served the engineering community for many years.

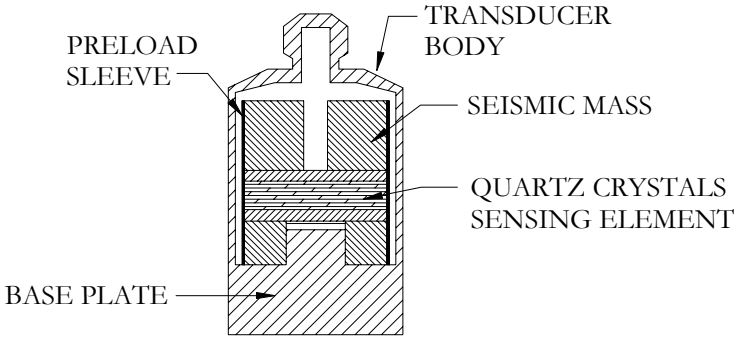

Figure 2.8 - Schematic Diagram of a Typical Accelerometer

- **Disadvantages**: Conventionally defined modal parameters have been shown by many to not be sensitive enough to detect many types of bridge damage. Furthermore, the modal parameters of conventional modal testing are global parameters that cannot define specific locations of damage. There also may be a high level of noise with the diagnostic signals associated with accelerometers.

2.3.5.8 Linear Variable Displacement Transducers (LVDT)

The basic structure of an LVDT is a series of inductors in a hollow cylindrical shaft and a solid cylindrical core (Figure 2.9). The LVDT produces an electrical output

proportional to the position of the core (FLW, 1997). The LVDT may be used in many different types of measuring devices that need to convert changes in physical position to an electrical output. The lack of friction between the hollow shaft and the core prolong the life of the LVDT and enable very good resolution. In addition, the small mass of the core allows for good sensitivity in dynamic tests. Most commonly, a LVDT is used to measure weight, pressure, torque, and similar phenomena, by sensing the deformation of calibrated beams, diaphragms, or other components to which mechanical force is applied.

The LVDT is constructed with two secondary coils placed symmetrically on either side of a primary coil contained within the hollow cylindrical shaft (Collins Corp., 1997). Movement of the magnetic core causes the mutual inductance of each secondary coil to vary relative to the primary, and thus the relative voltage induced from the primary coil to the secondary coil will vary as well. Because the two voltages are of opposite polarity, the secondary coils are connected in series opposing in the center, or Null Position. The output voltages are equal and opposite in polarity and, therefore, the output voltage is zero. The Null Position of an LVDT is extremely stable and repeatable. When the magnetic core is displaced from the Null Position, an electromagnetic imbalance occurs. This imbalance generates a differential AC output voltage across the secondary coils, which is linearly proportional to the direction and magnitude of the displacement.

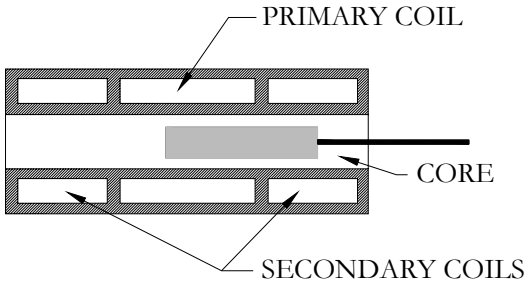

Figure 2.9 - Schematic Diagram of a LVDT

- **Advantages**: Advantages of LVDTs are the inherent ruggedness and durability of a transformer and provide infinite resolution in all types of environments. As a result of the superior reliability and accuracy of LVDTs, they are the ideal choice for linear motion control.
- **Disadvantages**: A disadvantage of a LVDT is the size of the LVDT, which could be a problem in tight areas and situations that require smaller sensors.

2.4 Summary

Non-destructive evaluation and structural health monitoring have been discussed in this chapter. The techniques have many similar advantages to monitor the performance of the KDOT fiber composite bridges:

- Both techniques will not damage the structure.
- Both techniques can be used without shutting down the structure.
- Both would provide a feasible way to monitor the behavior of the KDOT fiber composite bridges.
- Both monitoring techniques can incorporate a number of different sensors to acquire several measurements, and use mostly the same instrumentation.

The type of sensor chosen will play an important role in the longevity of the structural system. The combination of these sensors and monitoring techniques will create a reliable

method to monitor the performance of the structure. There are multitudes of different sensors that have applications for several different industries. Sensors can be used alone or in a series or network. The right sensor must be chosen based on the parameter that needs to be measured. Table 2.2 provides a list of sensors and how they might apply to the KDOT FRP composite bridge.

To select an appropriate monitoring technique, understanding of the structural systems is required. The locations where problems may exist must be identified so that the implementation of the sensor and monitoring technique can yield good results. The way the sensors are installed also plays a large role in how accurate the measurements are.

Table 2.2 – Sensors and How They Apply to the KDOT Bridge

Sensor	How They Apply to the KDOT Bridge
Fiber Optics	Can be used as strain gages and permanently bonded to the structure, which are corrosion resistance. Then they can be used to collect measurements at any time reducing installation costs.
Fiber Bragg Grating Strain Sensors	Same reason as above except these sensors can be linked together be a single fiber optic strand and there is no need for a light source.
Piezoelectric Transducers	Can be used to measure deformation on parts of the bridge. However, excessive vibration due to the FRP deck can lead to significant noise and poor results.
Strain Gages	Good for temporary results. Permanently bonding sensor to structure can alter accuracy of the measurements over time due to environmental effects and hysteresis.
Acoustic Emission	Can be used in areas of the bridge to determine the structure integrity of the FRP composite deck. Acoustic emission can help detect if delamination of the composite has occurred.
Micro-sensors and MEMS	Extremely expensive and beyond the scope of the bridge
Accelerometers	Can be used to check if any changes have occurred in the frequencies of the modal shapes. This would suggest a change in the physical properties of the bridge, which could be attributed to damage.
Linear Variable Displacement Transducers	Can be used to measure displacement in the bridge if it is desirable.

Chapter 3

Finite Element Models

3.1 Introduction

Chapter 3 gives a description of two Finite Element, FE, models that were created to help estimate the long-term behavior of the KDOT FRP bridge. This chapter also details decisions in regard to selection of appropriate finite element models. The decisions concern selection of elements, the boundary conditions, and the geometry and location of the components of the model.

3.2 Finite Element Software

All finite element models were created using the program ANSYS/Faculty Research Edition 5.5, developed by Swanson Analysis Systems of Houston, PA (2000).

3.2.1 Meshing

ANSYS has the features of free and mapped meshes. Free meshing allows the software to determine the best arrangement and pattern of the elements and the user chooses the fineness of the mesh. Mapped meshing allows the user to have complete control on the arrangement and pattern of the elements. Mapped meshes are more desirable for large models. Locations of the bridge that require a finer mesh can be used with locations that do not require a fine mesh. This optimizes the use of elements, and was therefore the technique used for this study.

3.3 Finite Element Models

There were two finite element models developed to help predict the behavior of the KDOT FRP bridges. The first model, referred to as the main model, was developed to simulate the behavior of the bridge as a whole. The main model consisted of a small tributary portion of the entire

length of the bridge. The second model, referred to as the submodel, was developed to examine the behavior of the connection between the steel wide-flange beam, FRP saddle beam, and FRP deck panel. The submodel consisted of only a small portion of the main model, with the addition of the detailed components of the connection. Submodeling is a finite element technique used to get more accurate results in a particular region of the model, which in this case, was the connection area. Submodeling uses the displacements generated from the main model to apply to the submodel.

3.3.1 Main Finite Element Model

The main finite element model was developed to provide an overall assessment of the bridge. From the data generated, the displacements, strains, mode shapes, and the contribution of the FRP deck could be examined. The analyses of the main FE model revealed regions of high stress or strain.

3.3.1.1 Modeling

Developing a detailed FE model of the entire bridge was not practical because of the demands for modeling time and processing power. With this limitation, the main FE model was created as a small tributary portion of the bridge. To make sure the small tributary portion of the bridge would behave similar to the entire bridge, symmetrical boundary conditions were used on the sides of the FRP deck. Symmetrical boundary conditions force the model to behave like a series of identical cross-sections by creating the same tributary portion on either side of the boundary surface.

The tributary portion of the bridge consisted of a single W21X68 steel wide-flanged beam, neoprene pad, FRP saddle beam, and a tributary width of the FRP deck panel. Figure 3.1 illustrates the four different components of the main FE model.

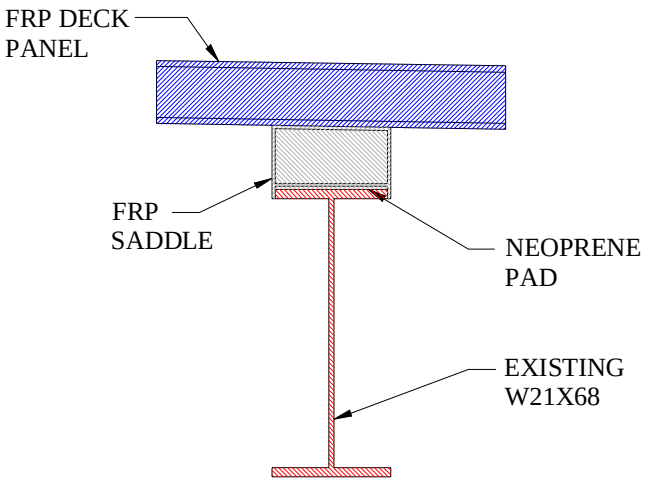

Figure 3.1 - Schematic Break-down of the Components of the Main Model

The FRP saddle beam and FRP deck panel consist of two parts: polyester resin and E-glass to form a fiber-reinforced polymer composite. The core of the FRP saddle and the FRP deck panel is made up of a honeycomb pattern of FRP composite, which consists of only a small percentage of FRP composite by volume. The top and bottom portion of the FRP saddle and FRP deck consist of laminated plates having approximately 50% E-glass by weight. Because the amount of FRP composite within the core was proportionally small compared to the laminated plates of FRP composite, assumptions had to be made on the stiffness of the overall core. A conservation approach was used and the entire volume of the core was assumed to consist of polyester resin (Figure 3.2).

Modeling the thin laminated plates of the FRP composite posed many problems. The honeycomb pattern of the core within the FRP saddle and deck consisted of many thin sheets of FRP composite with a thickness of approximately 6 millimeters. The top and bottom portion of the FRP saddle and deck consisted of laminated FRP composite plates of approximately 12 millimeters in thickness. Because the thickness of the core and the laminated plates were

relatively small with respect to the overall length of the bridge, modeling these components using three-dimensional solid elements was impractical, too costly and would required an enormous number of elements just to meet aspect ratio restrictions. The default aspect ratio in ANSYS for three-dimensional solid elements was 20:1. This would limit the largest element length to 120 millimeters for the web, which was only 6 millimeters thick. Because the overall length all the bridge was approximately 14 meters, the number of elements throughout the length of the model could not be less than 117. The version of ANSYS that was used was limited to only 120,000 degrees of freedom, which is directly related to the number of elements. Both the aspect ratio limitation and the degree of freedom limitation set the criteria for the size of the main FE model. These restrictions encouraged consideration of other element possibilities.

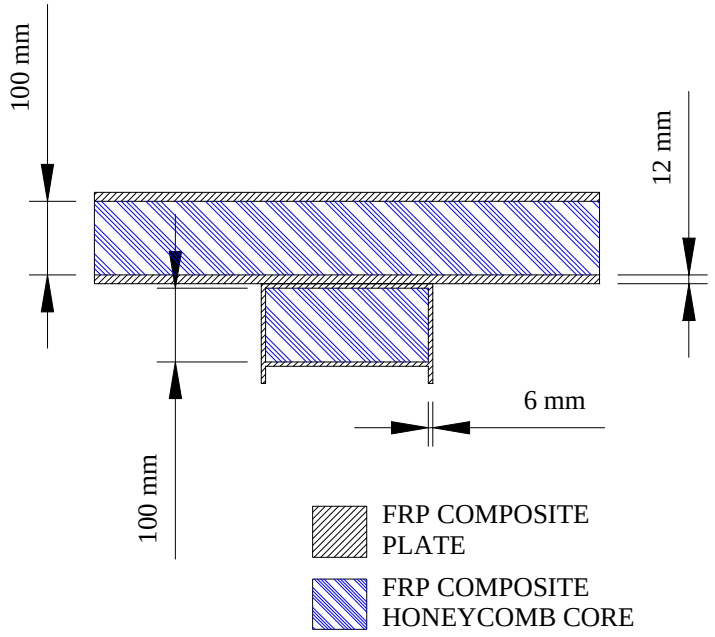

Figure 3.2 - Dimensions and Materials of the FRP Saddle and FRP Deck Panel

Several other options were examined for creating the model. There were essentially three ways to create this model: model with areas, model with volumes, or model with a combination of areas and volumes. As previously stated, modeling with volumes has limited application.

Modeling the entire model in three-dimensions with areas would solve the aspect ratio limitations, but the honeycomb pattern of the deck and saddle beams core created modeling difficulties. Using a volume to represent the core could be created to behave similar to the honeycomb pattern of the FRP composite and would simplify the model considerably. Lastly, if the model was created using a combination of volumes and areas, this could solve both limitations, but there would be some element compatibility issues as described below.

Compatibility problems between degrees of freedom, DOF, of certain elements were introduced when using a combination of volumes and areas. A solid brick element was selected to mesh the volumes and a shell was selected to mesh the areas. Incompatibility arose as a typical shell element contains six degrees of freedom (xyz displacements and xyz rotations), whereas a typical brick element has three degrees of freedom (xyz displacements). Combining these two elements would decrease the amount of nodes and elements of the main model, make modeling more efficient, and decrease the required processing power. However, connecting a three DOF element to a six DOF element requires a transition element to preserve all original DOFs modeled. Although there are many other elements to choose from, such as brick elements with rotations, which would increase the number of degrees of freedom, it was more desirable to use only one type of element. Therefore, all of the components of the main model were meshed using solid brick elements. Meshing entirely of volumes in three-dimensional space assured DOF compatibility between all components of the model. In addition, the sub model implements contact elements with three DOF (xyz displacements) and further supported the selection of solid brick elements.

Some of the physical dimensions (Figure 3.3) and properties of the constructed bridge were simplified for the model:

- The honeycomb pattern of the saddle beam and deck panel was modeled as a single volume using the properties of the polyester resin, which provided a similar stiffness to the actual condition.
- All edges that were rounded in the physical bridge were squared in the model.
- In the main model, all of the components are modeled together as a bonded section, which differs from the actual bridge and is discussed later in chapter 4.

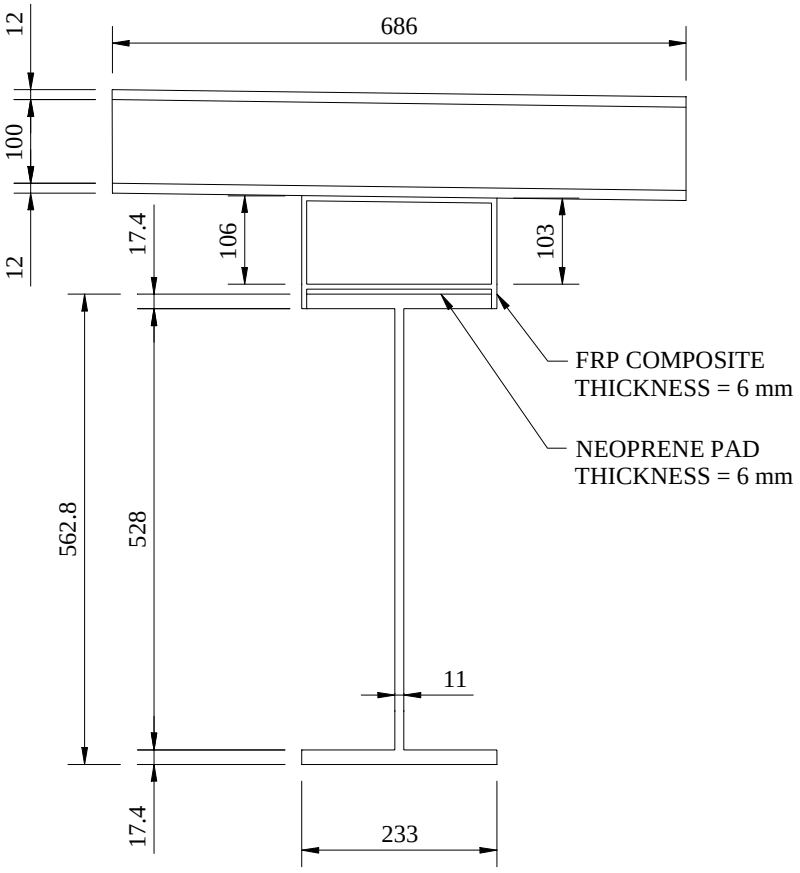

Figure 3.3: Dimensions of the Main FE Model

(Dimensions are in Millimeters)

- The slope of the bridge for drainage consideration was incorporated into the model.
- The steel nosing at each support was ignored because it did not contribute to the long-term behavior of the bridge.
- A void was created within the FRP deck core to represent the discontinuity at the bolted connections (Figure 3.4).
- The existing steel girder at the supports was extended beyond the saddle beam and deck and fully restrained to mimic the steel girder embedded into the abutment (Figure 3.4).

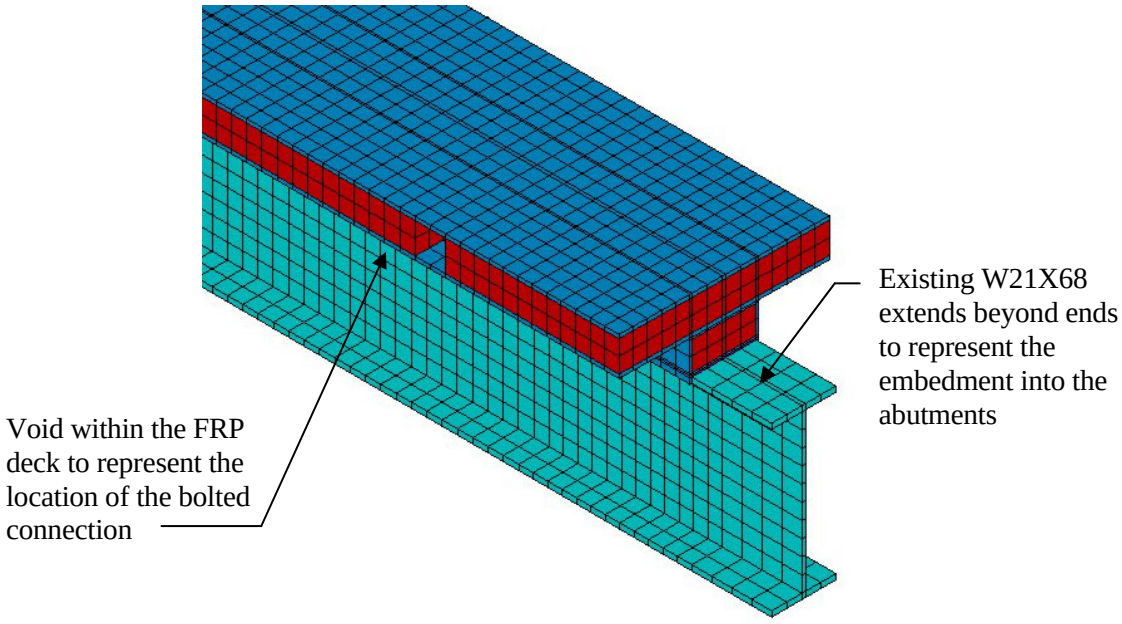

Figure 3.4: Illustration Showing the Two Variations in the Main FE Model

After the cross-section dimensions and geometry of the model were determined and the modeling issues resolved, the coordinates of the key points, or nodes, were mapped into the model. From these key points, the volumes were created and then the elements. Typically, using 20-noded solid brick elements to mesh volumes yield better results. However, because of the

enormous number of elements needed to mesh the main FE model due to aspect ratio limitations, 8-noded solid brick elements would provide sufficient accuracy for the desired results.

3.3.1.2 Materials

Orthotropic material properties were used in both the main model and submodel to represent the tri-directional properties of the FRP composites. Table 3.1 lists the material properties for each component. The properties of the FRP composites were provided by KDOT and typical properties for steel and neoprene were selected for the model.

Table 3.1: List of Materials Properties Used with Finite Element Models

Property	Materials			
	Mild Steel	FRP Composite	Polyester Resin	Neoprene Rubber
E_x (MPa)	200000	50000	3500	2
E_y (MPa)	200000	15200	3500	2
E_z (MPa)	200000	15200	3500	2
γ (kg/mm^3)	8.03E-06	2.50E-07	1.50E-07	2.00E-06
α_x (/deg C)	1.17E-05	6.34E-06	2.33E-05	1.00E-04
α_y (/deg C)	1.17E-05	2.33E-05	2.33E-05	1.00E-04
α_z (/deg C)	1.17E-05	2.33E-05	2.33E-05	1.00E-04
γ_{yz} (Mpa)	76925	20000	1306	0.67
γ_{xz} (MPa)	76925	5325	1306	0.67
γ_{xy} (MPa)	76925	6060	1306	0.67
ν_x	0.3	0.254	0.34	0.49
ν_y	0.3	0.34	0.34	0.49
ν_z	0.3	0.254	0.34	0.49

In addition to the material properties listed in Table 3.1, all materials were assumed to have a coefficient of friction of 0.3, which was needed for the contact elements in the submodel analyses. For the analyses considering temperature differentials, a reference temperature of zero degrees Celsius was used.

3.3.2 Sub Finite Element Model

The sub finite element model was developed to provide a more detailed assessment of the bolted connection between the steel girder, FRP saddle beam and FRP deck panel. Because the bolted connection had many components that could not be modeled in the main model, the submodel was used to examine the behavior of those components. Contact elements were used in the submodel to model the friction between the components, which were impractical in the main model due to size and storage limitations. From the data generated, the stresses, strains, displacements, and the interaction between the FRP composites and the existing steel girder could be determined with greater precision. From the analyses of the main FE model, portions of the main model that exhibited large stresses or strain were selected for further examination with the submodel. Two portions were submodeled: the bolted connection closest to the support, and the bolted connection closest to the midspan (Figure 3.5).

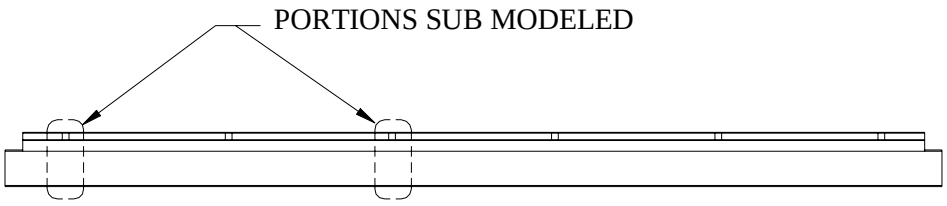

Figure 3.5: Locations of the Bolted Connections that were Sub-modeled

3.3.2.1 Modeling

Because the geometry and components of the two submodels were identical with the only differences in the location and the displacements applied from the main model, only one FE submodel was created. The illustration in Figure 3.6 (provided by KDOT) describes the bolted connection and all of the structural elements. All of these structural elements were included in the submodel so that the behavior of the assembly could be determined. Development of the submodel also included the clamping plates and bolts with a prestressing force to simulate the tightening of the bolt. Because the actual pretensioning force in the bolt could not be determined due to unknown factors, such as environmental effects, a corresponding force in the bolts was determined from AISC design recommendations (described below).

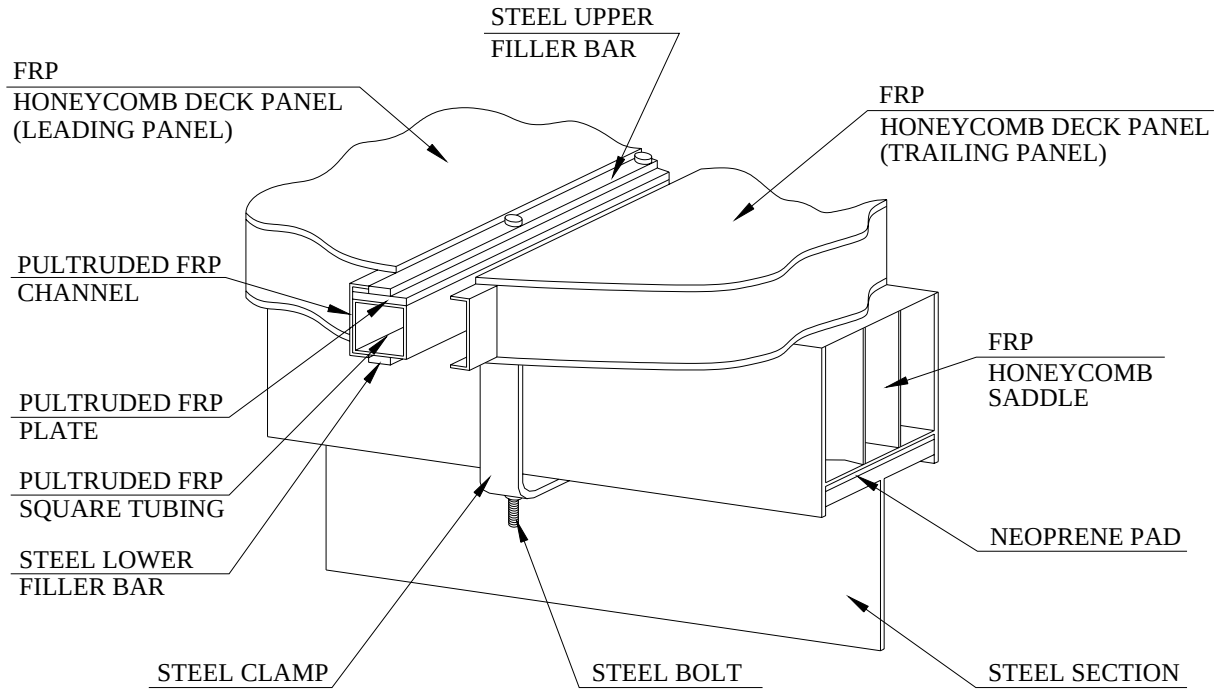

Figure 3.6: Isometric Drawing of the Bolted Connection

Similar to the meshing problems encountered with the main model, the relative thickness of the structural connection components were small compared to the rest of the model. This would require a finer mesh, and therefore only a small portion of the main model was included. The entire length of the submodel was only 500 mm, approximately $1/30^{th}$ the size of the main model. The smaller size of the submodel meant that more elements could be used without violating element limitations and greater precision could be obtained.

The volumes were strategically mapped out, so that a finer mesh could be used in the bolt and connection components within the deck panel where the highest stresses were calculated. The bolt in the model produced aspect ratio problems, and governed the mesh size. However, some portions of the model around the bolts could not be reasonably meshed without having element aspect warnings. Because the bolts were only connected at the top of the deck panel, holes 1 mm larger than the bolt were created between the bolt and the beam. This 1 mm sliver around the bolts had to be mapped throughout the model, so that the alignment of the nodes would not create any problems with connecting degrees of freedom between elements. Over 2600 volumes were individually created within the submodel, which required careful planning so that all of the nodes would match once the volumes were meshed (Figure 3.7). Using an aspect ratio of 20:1 for all volumes was not possible and would have increased the model beyond the limits set within ANSYS. Therefore, some aspect ratio warnings existed within the model. However, this did not affect the accuracy of the results.

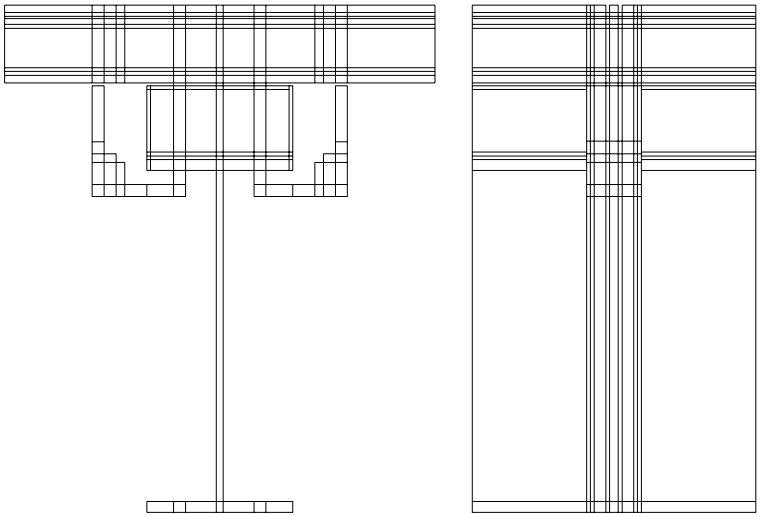

Figure 3.7: Submodel Volume Alignment

In addition to the alignment causing modeling difficulties, the contact elements between the deck panel and saddle beam had to be carefully mapped. Contact elements were useful to model the interaction of two surfaces. This was very important in determining the behavior between the steel girder and saddle beam, and the saddle beam and deck panel. With the addition of contact elements, the amount of composite action could be determined and the affect of sliding between surfaces could be included. Sliding between surfaces could cause significantly higher stresses such as due to shearing of the bolts. Contact elements have conditional physical properties, such as tangential and normal stiffness, which can be modified so that the amount of slip or friction between the components can be determined (Figure 3.8).

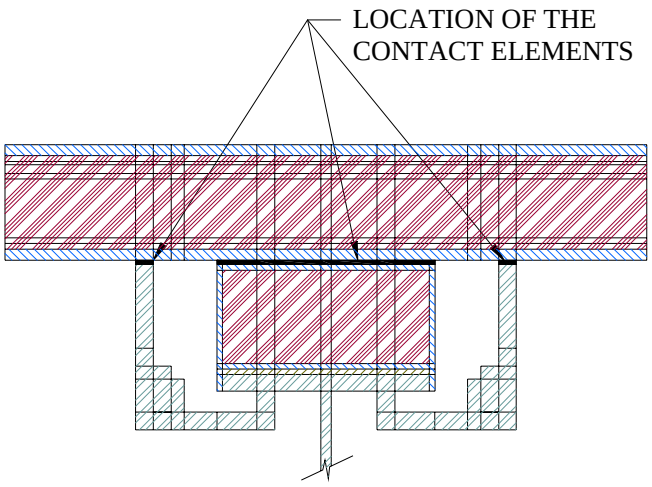

Figure 3.8: Location of the Contact Elements

To use contact elements, a non-linear analysis was required. One of the most difficult problems with contact elements was to determine the normal stiffness. Because the normal stiffness can range from a few hundred MPa to several million MPa, a series of analyses were conducted to select the appropriate stiffness by convergence of the solution. The normal stiffness that was selected for the final analyses was 500 MPa. To determine the tangent stiffness, the default recommended value from ANSYS, KT = KN/100, was used. The friction behavior was calculated using the rigid Coulomb friction model, which uses equivalent shear stresses to determine slip.

To model the prestressing force within the bolt, a temperature differential was applied to the elements of the bolt. The force within the bolt was created using a torque wrench rated at 135 kN-mm. Because an exact correlation between the tension force and the applied torque could not be determined (i.e. the manner that they were installed, the temperature when they were installed, etc.), AISC design recommendations were used. For a 16 mm A325 bolt, the minimum bolt tension is 85 kN. To achieve this force, a temperature differential of -183.5 °C was applied. Because there was an initial gap of 0.1 mm between the saddle beam and the deck

panel, an additional differential of -29.5 °C was applied. Therefore, the total temperature differential applied was -213 °C.

Applying a temperature differential to the elements within the bolts had some limitations. It could not model the physical behavior exactly and the stress at the ends of the bolts was misleading and inaccurate. Other methods for applying the prestress force were examined, such as equal and opposite loads within the bolts. This method provided good results at the location of the load, but inaccurate results toward the ends and middle of the bolt. The temperature differential provided the most accurate clamping force for the connection and had the least variation in the stress throughout the bolt. This method would provide the correct behavior of the bolts and not alter the conclusions. However, the stresses within the bolts should be ignored.

3.4 Summary

In this chapter, the main and sub finite element models that were created to help predict the long-term behavior of the KDOT fiber composite bridge were explained. This chapter discussed specific decisions in regard to selection of appropriate finite element models and the decisions concerned with the selection of elements, boundary conditions, geometry, and location of the submodels.

- **Main Model**: The main finite element model was created entirely of eight-noded three-dimensional solid brick elements using ANSYS. The main model incorporated:
    - Symmetrical boundary conditions.
    - Voids to represent the discontinuity at the bolted connections.
    - Fixed supports.
- **Sub Model**: The sub finite element models were created entirely of eight-noded three-dimensional solid brick elements using ANSYS. The sub model incorporated:
    - Symmetrical boundary conditions.

- All of the components within the bolted connection.
- Contact elements to model friction between the deck, saddle, and girder.
- Prestressing force within the bolts based on AISC recommendations.

Chapter 4

Analyses

4.1 Introduction

Chapter 4 discusses the results of the finite element analyses as well as the data gathered from the non-destructive testing of the bridge. This chapter discusses each analysis as to why it was used, and what assumptions were made. The chapter also illustrates the stresses and strains determined by the finite element models.

4.2 Reliability of the Finite Element Models

An important task in this study is to gage the reliability of the finite element models to predict the actual behavior of the bridge. A previous study of the bridge (Schreiner, 2000), which involved non-destructive evaluation using strain gages, provided information on the performance of the bridge. From the data collected, the stresses from the finite element models could be verified.

The first set of data recorded is from a truck weighing approximately 212 kN. The strain gages were located on the bottom flange of the steel girder at the midspan. The stress was calculated from the strain recorded at these locations. The 212 kN truck was driven across the bridge at various speeds ranging from a "crawl speed" to approximately 80 km/h. The lowest stress, approximately 22 MPa, occurred due to "crawl speed loading," whereas the highest stress, approximately 24 MPa, occurred due to 80 km/h loading.

The total weight of the AASHTO HS-25 design truck used for the finite element models was approximately 405 kN. The highest stress observed at the midspan from the main model, using a similar loading pattern, was approximately 48 MPa. Proportioning the stress from the

main model to the test truck resulted in a stress of approximately 25 MPa. This stress is within 4 to 12 percent of the actual stress in the bottom flange of the steel girder at the midspan.

4.3 Analyses

There were three types of analyses performed: a modal analysis, static analysis, and non-linear analysis. The modal analysis calculated the modes and frequencies of vibration for the tributary portion of the bridge modeled. Comparing the modes and frequencies calculated from the modal analysis to the frequencies generated from the accelerometers of the non-destructive testing of the bridge, provided a way to determine if problems could occur due to vibration. The static analysis was a simple way to determine the stresses, strains, and displacements within the main finite element model. The non-linear analysis was used to calculate the contact element behavior for the submodel.

4.3.1 Modal Analyses

Two types of modal analyses were performed: one using non-destructive testing (experimental) of the KDOT fiber composite bridge to record measurements on vibration and another using a FE analysis to calculate the modes and frequencies of vibration of a tributary portion of the bridge (analytical). The modal analyses were primarily used to determine if significant composite action developed between the girder and FRP composite saddle and deck and to compare frequencies from the FE analysis to the frequencies of the non-destructive testing.

Non-destructive testing was conducted using accelerometers that were bonded to the underside of the girders and FRP deck. The accelerometers were attached at three locations: quarter span, one-third span, and midspan. Several traffic patterns were used to determine the effects of direct and indirect loading. The electrical signals generated by the accelerometers

were gathered and stored in a notebook computer to be used with software (EASE, 1999) to extrapolate the data. Figures 4.1 and 4.2 describe the frequency response of the girder and deck respectively at the middle of the structure. Figures 4.3 and 4.4 describe the frequency response of the girder and deck respectively at the quarter span.

The spectrum responses for both the deck and the girder illustrate the differences in the vibration patterns. The girder dissipated most of the energy at low frequencies with a peak frequency around 50 Hz. The deck dissipated the energy evenly across a broad frequency range with a peak frequency around 160 Hz. This difference in energy dissipation suggests the deck and girder behave independently. The deck deflects from beam-to-beam, whereas the girder deflects from support-to-support.

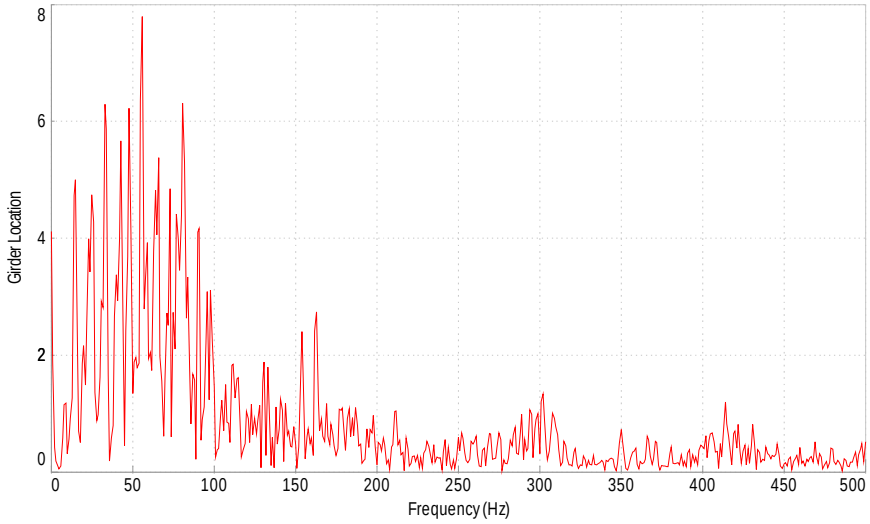

Figure 4.1: Spectrum Response at the Midspan of the Existing Steel Girder

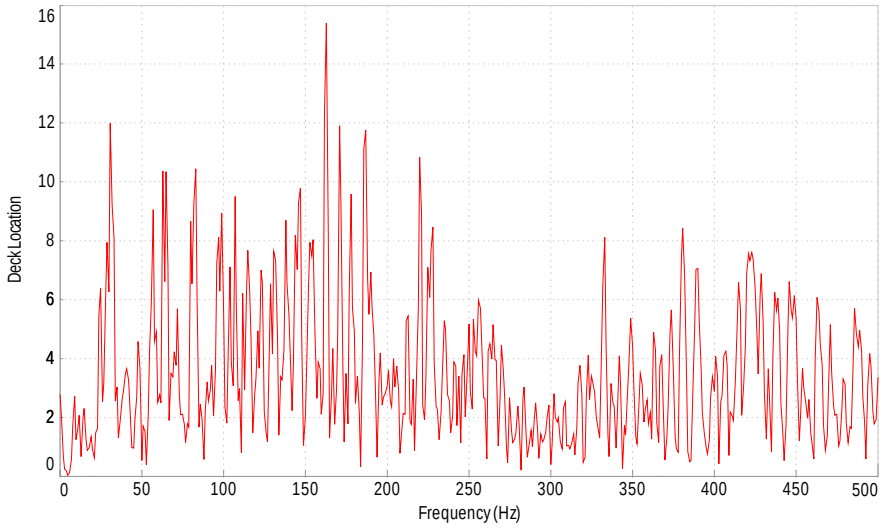

Figure 4.2: Spectrum Response at the Midspan of the FRP Composite Deck

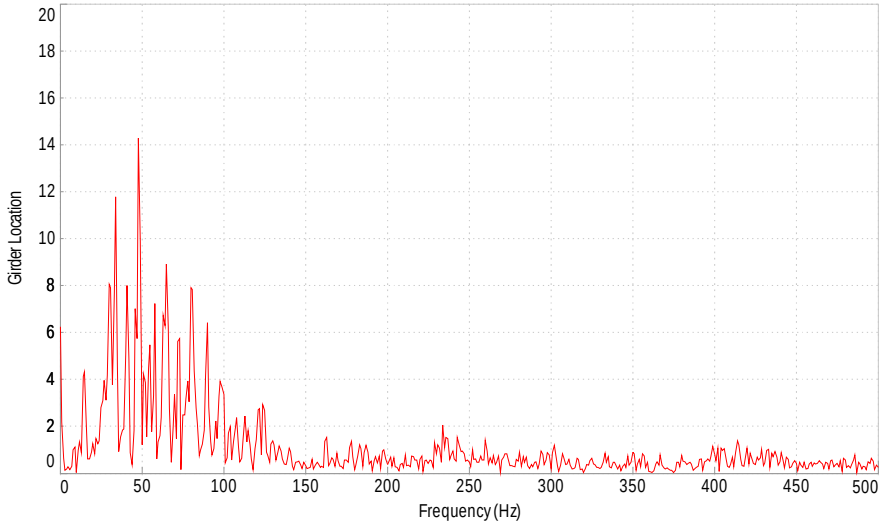

Figure 4.3: Spectrum Response at the Quarterspan of the Existing Steel Girder

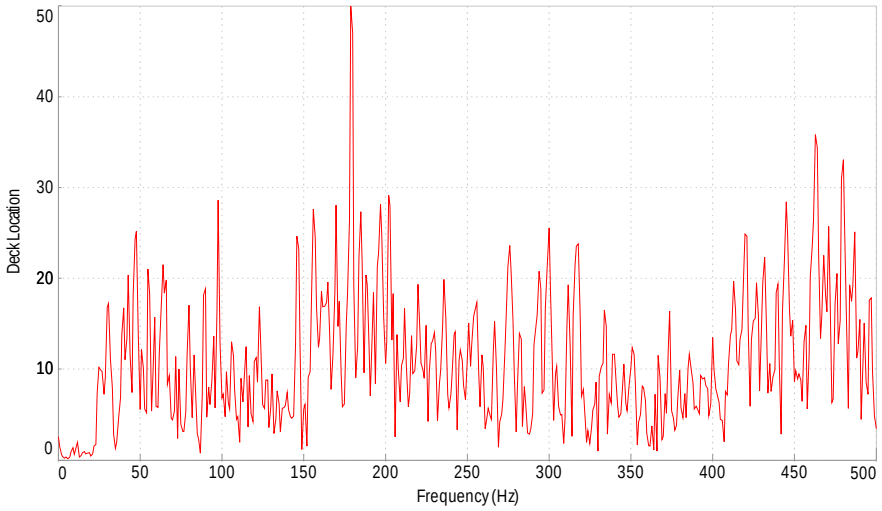

Figure 4.4: Spectrum Response at the Quarterspan of the FRP Composite Deck

The modal analysis of the FE model provided the modes and frequencies of a tributary portion of the bridge, which could be compared with the experimental data. Figure 4.5 illustrates two vertical mode shapes and the associated frequency of the modal analysis from the FE model.

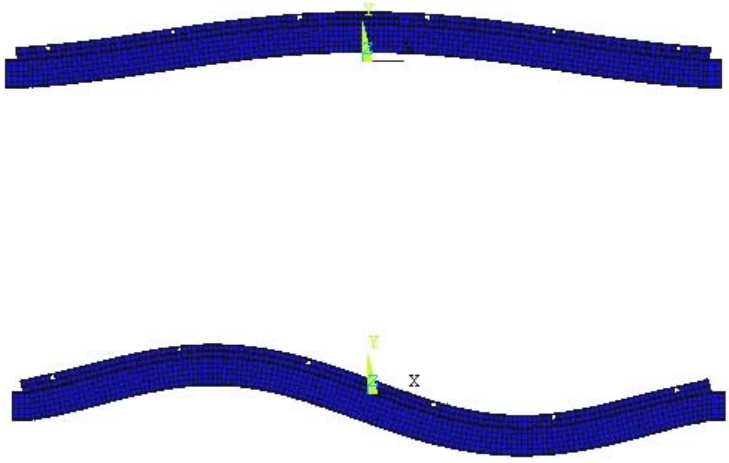

Figure 4.5: Mode Shapes and Frequencies from the Main Finite Element Model

The first ten modal shapes were examined from the field study. The first ten mode shapes were in a frequency range between 0.25 Hz and 2.18 Hz. From the plotted mode shapes, the first vertical mode shape (single curvature) occurred at 0.79 Hz, and the second vertical mode shape (double curvature) occurred at 2.08 Hz. All other mode shapes were a result of torsion or bending about the weak axis. The mode shapes generated by the computer analysis illustrate the deck and girder deforming and behaving in unison. This was what was expected because the steel girder, FRP saddle and FRP deck were modeled together as one combined section. Comparing the experimental data with the FE analysis showed a significant difference in frequency range. This difference, however, does not have an effect on the FE model's ability to predict the stresses and strains of the bridge, because the loads are static (described later in this chapter). Instead, it suggests that the three main components do not exhibit the same behavior in all areas of the bridge. The main reason for the differences is due to the differences in stiffness between the steel girder and FRP composites, which play an important role in how energy is absorbed.

4.3.2 Static Analyses

A static analysis was used to solve the main finite element model. Rather than using contact elements to model the friction between the three main components (steel girder, FRP saddle beam, and FRP deck), the main FE model was created as a combined or bonded section. This allowed comparisons to be made with the experimental data gathered from the non-destructive testing and the submodel that utilized the contact elements. The solution of the main FE model provided the locations of the highest stress or strain, and indicated the best locations for the submodels. The solution also provided the displacements that would be used for the submodels. From this analysis, the amount of composite action could be extrapolated, and an

assessment could be made. This type of analysis provided an efficient way to calculate the capacity of the bridge, find out how much strength was attributed to the addition of the FRP deck, and locate any high stress concentrations throughout the bridge.

There were two different types of loads used for the static analysis: a mechanical and a thermal load. The mechanical load consisted of an AASHTO HS-25 design truck and the thermal load consisted of a temperature differential.

The analysis of the HS-25 truck was used to determine the contribution of the FRP deck to the overall strength of the bridge. To determine the relative amount of strength that was gained, the amount of composite action needed to be calculated. This type of analysis also helped to identify where the highest stresses were located throughout the bridge. The thermal load consisted of a temperature range of ± 15-20 °C. This analysis provided a method to determine the impact of fluctuating outside temperatures on the bridge. It was important to understand thermal effects of the bridge because the main materials of the bridge had different thermal properties.

4.3.2.1 AASHTO HS-25 Design Truck

The HS-25 design truck consisted of three axle loads. The design load for the middle and rear axles were 45 kN, whereas the design load for the front axle was 11 kN. According to AASHTO, the distance between the front and middle axles was 4.3 meters, and the middle and rear axles was 4.3 to 9 meters apart. It was determined that the spacing of the rear and middle axles that would produce the most critical loading condition was 4.3 meters and was used for all analyses.

Placement of the truck axle loads were chosen based on the following five critical forces or locations that also would provide the best assessment of the overall behavior of the bridge:

- Largest positive moment in the bridge.
- Largest negative moment in the bridge.
- Largest moment at the bolted connection closest to the midspan.
- Largest moment at the bolted connection closest to the supports.
- Largest shear in the bridge.

The location of the three truck axle loads that produced the largest positive moment in the bridge was similar to the location that produced the largest positive moment at the bolted connection closest to the midspan of the bridge. The location of the three truck axle loads that produced the largest negative moment and shear in the bridge also was similar to the location that produced the largest negative moment and shear for the bolted connection closest to the supports. Because several conditions were similar, it was determined that only two loading conditions were used in the analyses.

The first analysis (largest moment at the bolted connection closest to midspan) provided an accurate way to determine the contribution of the saddle beam and deck to the overall strength of the bridge and provided the displacements for a sub model of the bolted connection closest to the midspan. Figure 4.6 illustrates the loading that was used for the first analysis.

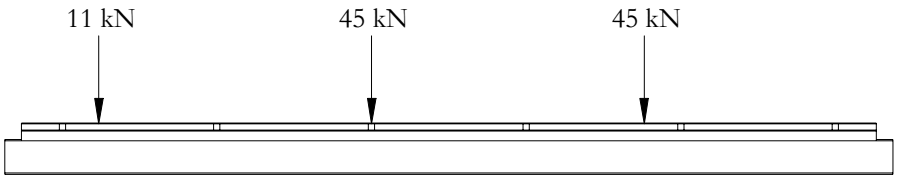

Figure 4.6: Location of Axle Loads for an AASHTO HS-25 Truck for the Bolted Connection Closest to the Midspan of the Bridge

The largest bending stresses (stress in the x-direction or along the length of the bridge), were found at the location of the bolted connection closest to the support and the bolted connection closest to the midspan of the bridge. Figure 4.7 is a plot of the Von Mises stress of the entire main FE model, which is an average of all three principal stresses and is considered as an accurate estimate of the actual stress. The general equation that describes the Von Mises stress is as follows:

$$\sigma_{vm} = \sqrt{[0.5*((\sigma_1 - \sigma_2)^2 + (\sigma_2 - \sigma_3)^2 + (\sigma_3 - \sigma_1)^2)]} \qquad (1)$$

where,

σ_{vm} is the calculated Von Mises stress

$\sigma_{1,} \sigma_{2,} \sigma_3$ are the principle stresses in the x, y, z directions respectively

The bending stress for the bolted connection closest to the support can be seen in Figure 4.8 (top) and shows a high stress concentration between the saddle beam and girder. Figure 4.8 (bottom) is a contour plot showing the bending stress of a portion of the main FE model near the bolted connection closest to the midspan of the bridge. Because the bolted connections provide a discontinuity within the FRP deck, it is reasonable that the stress would increase at these locations. However, the highest stress is in the bottom of the steel girder and the lowest stress is in the top of the deck. Figure 4.9 details the distribution of the bending stress throughout the section.

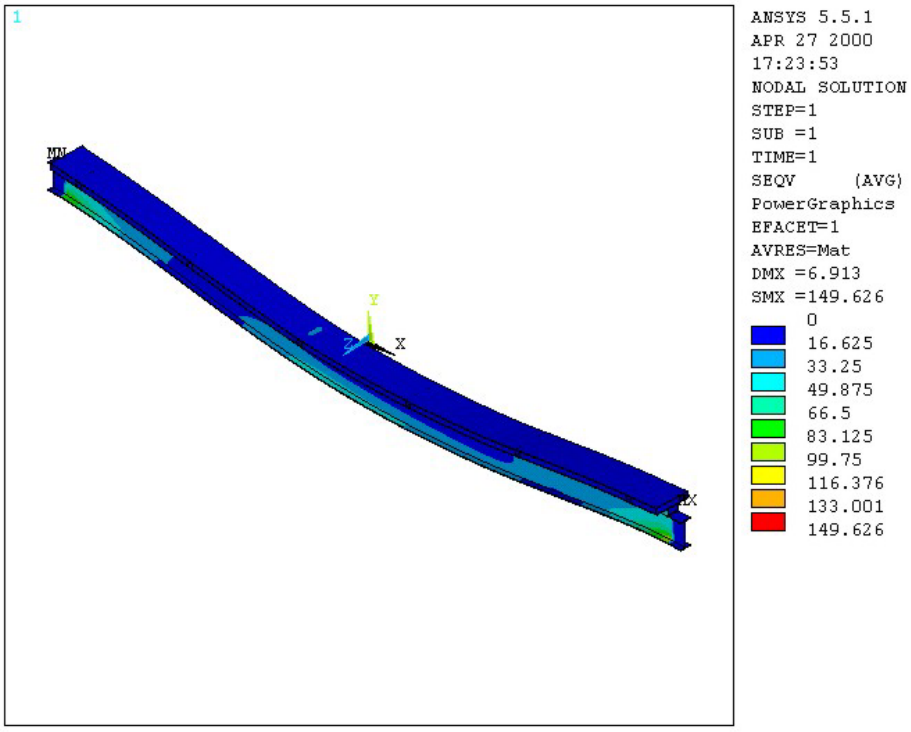

Figure 4.7: Plot of Von Mises Stress from the First Truck Loading Pattern

Figure 4.10 (top) is an isolated contour plot showing the bending stress of only the top of the FRP deck. This plot illustrates how much of the FRP deck contributes to the bending stresses. In the figure, the highest stress is within the center of the cross-section and decreases with increasing distance from the centerline of the cross-section. Figure 4.10 (bottom) is an isolated contour plot showing the bending stress of the bottom surface of the FRP deck. The area where the bottom of the FRP deck is in contact with the top of the FRP saddle beam there is a distinctive line where the stress changes drastically.

The second analysis was used to determine the impact of the largest negative bending and shear on the portion of the bridge closest to the support. Negative bending resulted from having the existing steel girders embedded into the abutments. The second analysis calculated the

displacements needed for the submodel of the bolted connection closest to the support. Figure 4.11 shows the location of the three axle loads used for this analysis.

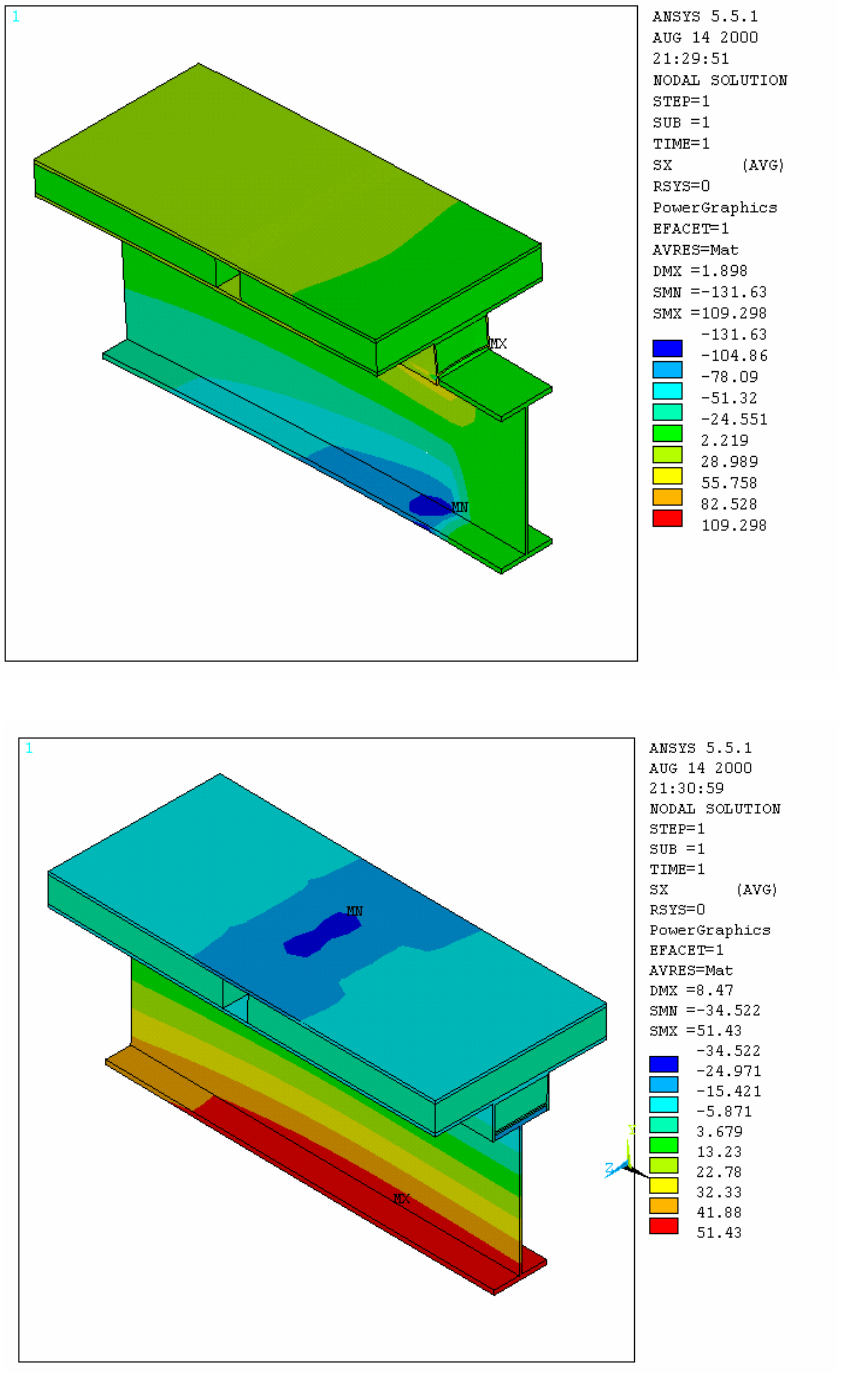

Figure 4.8: Plots of Bending Stress of the Bolted Connections Closest to the Supports and Midspan of the Bridge

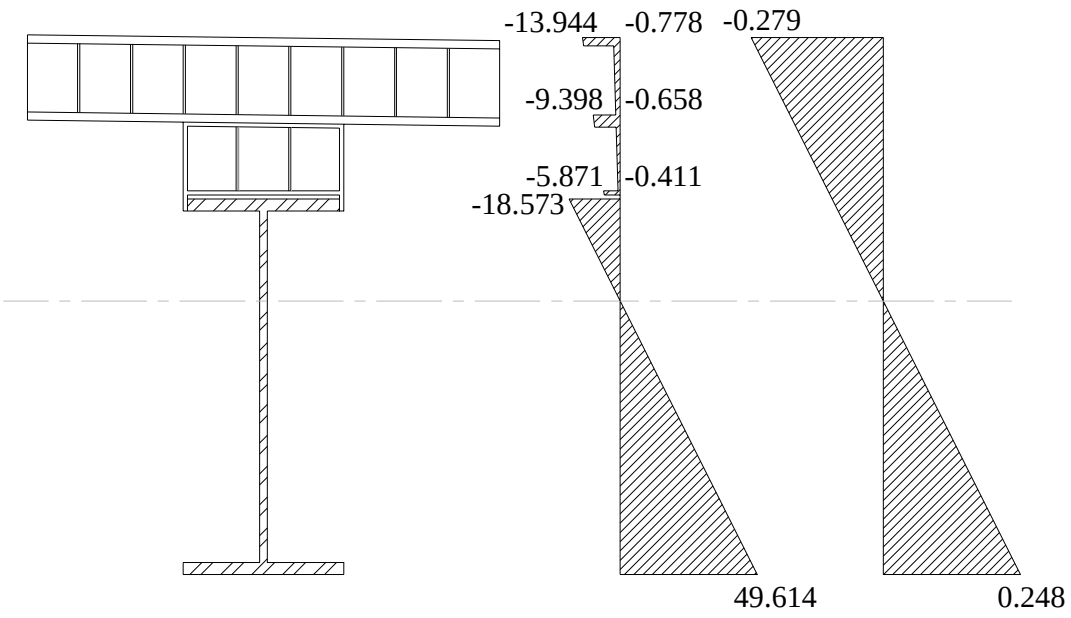

Figure 4.9: Diagram Showing the Bending Stress and Strain at the Midspan of the Bridge

The result of the second analysis was important because the area around bolted connection nearest the support experienced entirely different stresses than the area around the bolted connection closest to the midspan. Because the supports experienced negative bending, tension would develop within the FRP deck. If the stresses were large enough to pull the connection elements apart, dirt and grime could lodge into the joints between the deck panels. Although there was a ½ inch layer of polymer concrete overlay on the deck, the contribution was not accounted for in the analysis. Figure 4.12 (top) provides a contour plot of the bending stress for the portion of the bridge at the support.

A contour plot of the bending stress, Figure 4.12 (bottom), shows significant rotation of the FRP saddle beam and FRP deck at the support. This would be attributed to the lack of restraint on the deck and saddle beam because they are not embedded into the abutments like the steel girder. This rotation relieves the amount of tension in the deck and saddle beam at the supports.

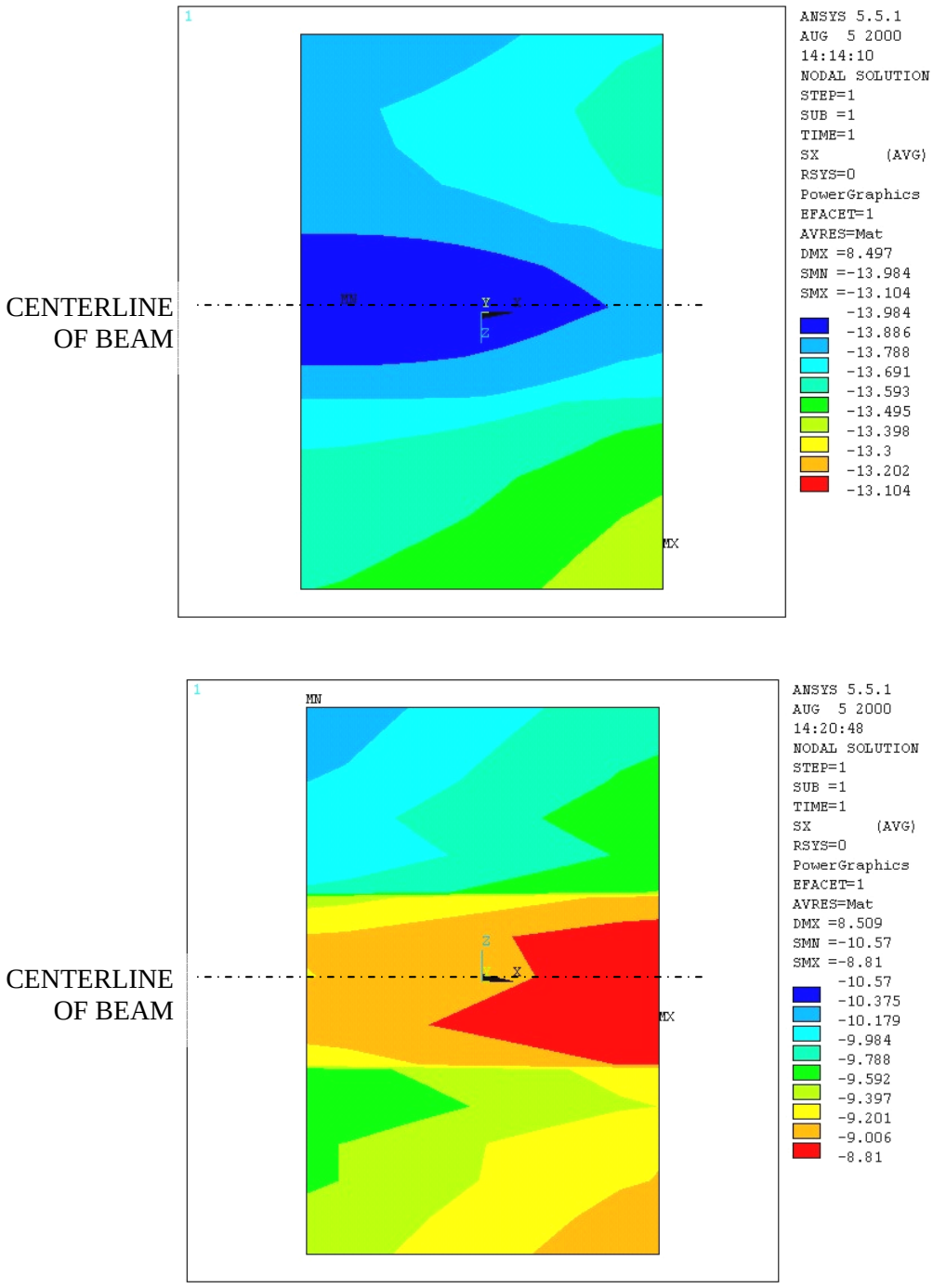

Figure 4.10: Plots of Bending Stress at the Top of the Fiber Composite Deck (Top) and Bottom of the Fiber Composite Deck (Bottom)

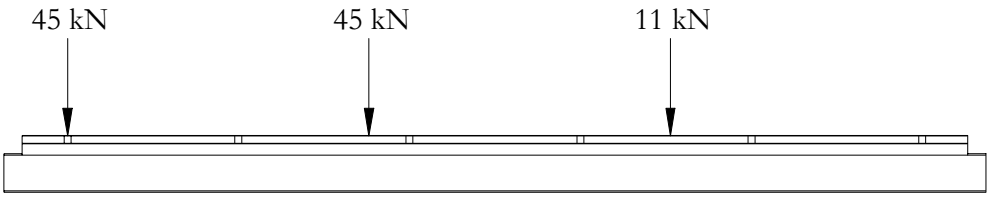

Figure 4.11: Location of Axle Loads for an AASHTO HS-25 Truck for the Bolted Connection Closest to the Supports

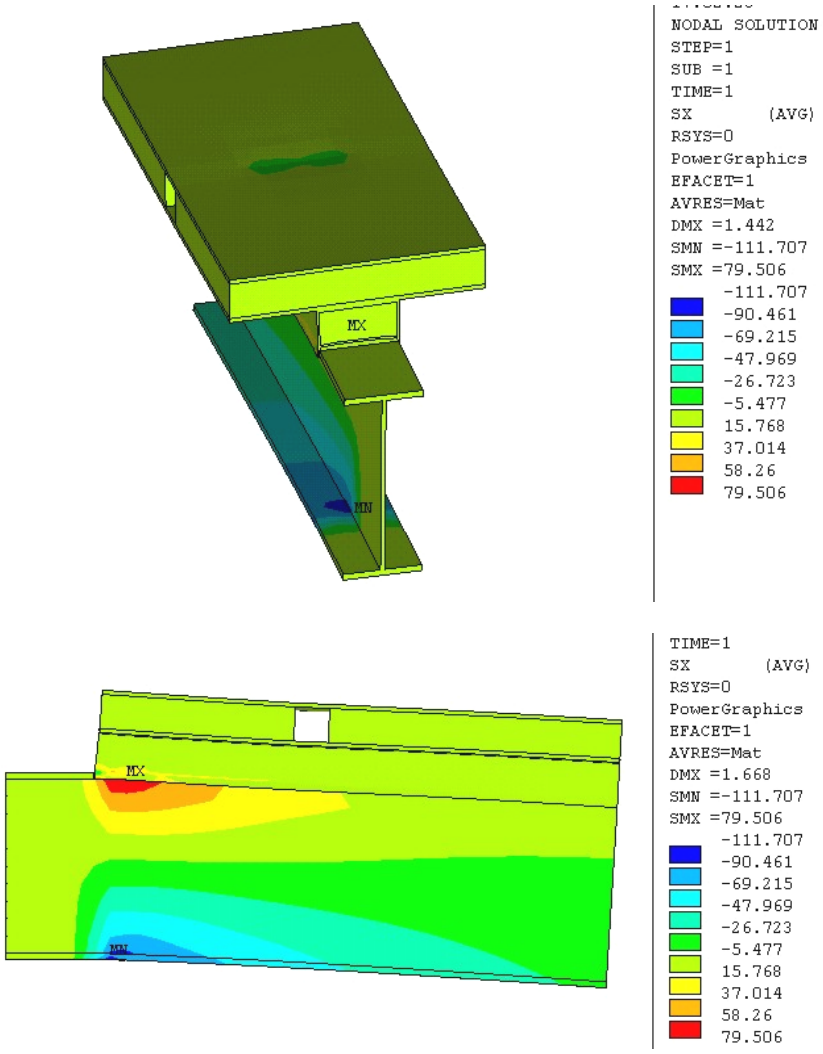

Figure 4.12: Plots of Bending Stress at the Supports under Traffic Loads

4.3.2.2 Temperature

Thermal effects on the bridge were analyzed. The combination of FRP composites and mild steel in a civil application such as the KDOT fiber composite bridges is a relatively new procedure and limited data is available on the behavior of this type of combination. The thermal coefficient of expansion for the FRP composites is about twice as large as that of mild steel (Table 3.1). The additional expansion or contraction of the FRP composites compared with the steel girder could produce negative effects.

New boundary conditions had to be implemented into the main FE model for the thermal analysis. The boundary conditions were placed on the ends of the saddle beam and deck in the x-direction to restrict expansion, due to the asphalt road. These boundary conditions were used only for a positive thermal differential.

There were two analyses used involving thermal differentials: an increase in temperature of 20 °C and a decrease in temperature of 20 °C. Figure 4.13 (top) shows a contour plot of the bending stress at one of the supports caused by an increase in temperature of 20°C. Although the stresses are relatively low and the deformation is grossly exaggerated, the highest stresses are along the construction joints, which is where the bolted connections are located. If these stresses are combined with stresses induced by truckloads, it could result in stresses exceeding the tensile strength of the polymer concrete overlay. Figure 4.13 (bottom) shows a contour plot of the bending stress at the midspan of the bridge.

The results from the analysis with a decrease in temperature are relatively the same except the stresses are opposite in direction. The highest stresses are at the supports between the saddle beam and the girder. Because in the actual bridge the FRP composites are not bonded to the steel girder, these stresses can be neglected. However, it is evident that bonding the three main components would introduce more stress at these locations. A negative thermal differential

causes the bridge to deflect downward at the midspan, similar to the deflection under truckloads. Because the supports do not restrict the ends of the saddle beam and deck from rotation, it is free to contract. Figure 4.14 (top and bottom) shows a contour plot of the bending stress caused by a decrease in temperature of 20°C.

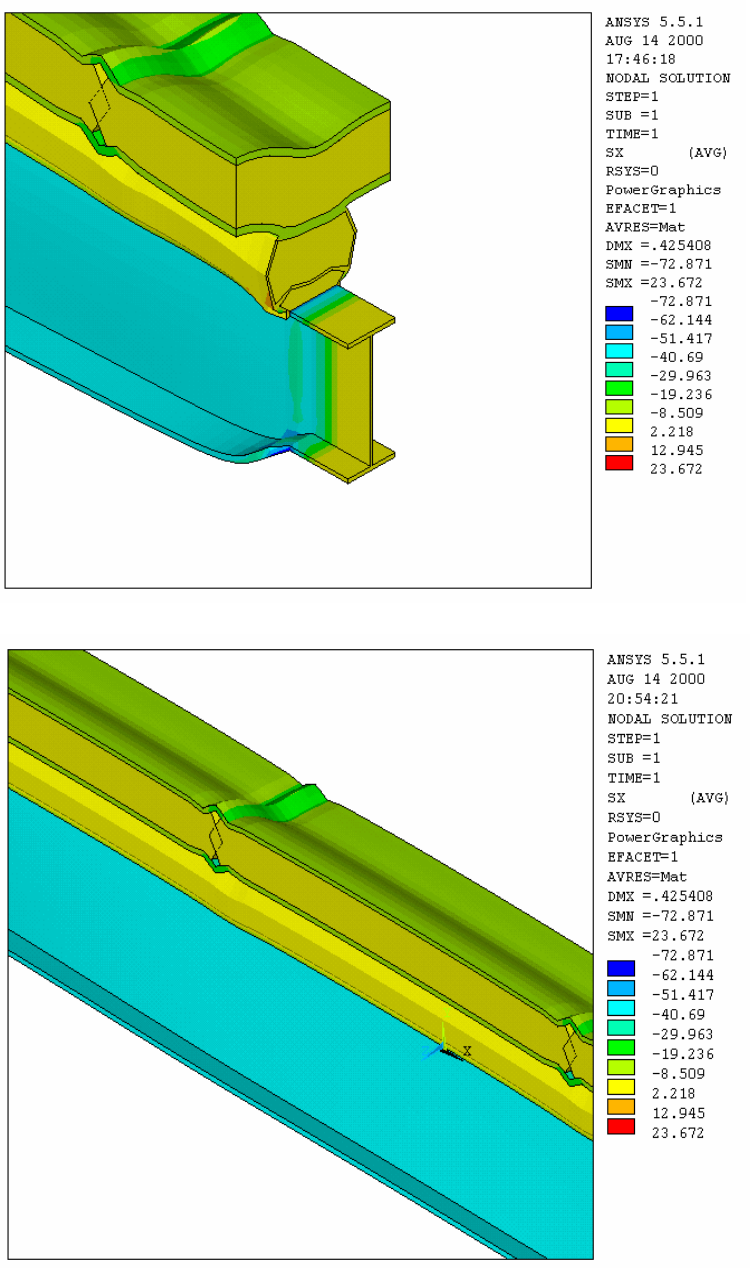

Figure 4.13: Plots of Bending Stress Due to an Increase in Temperature

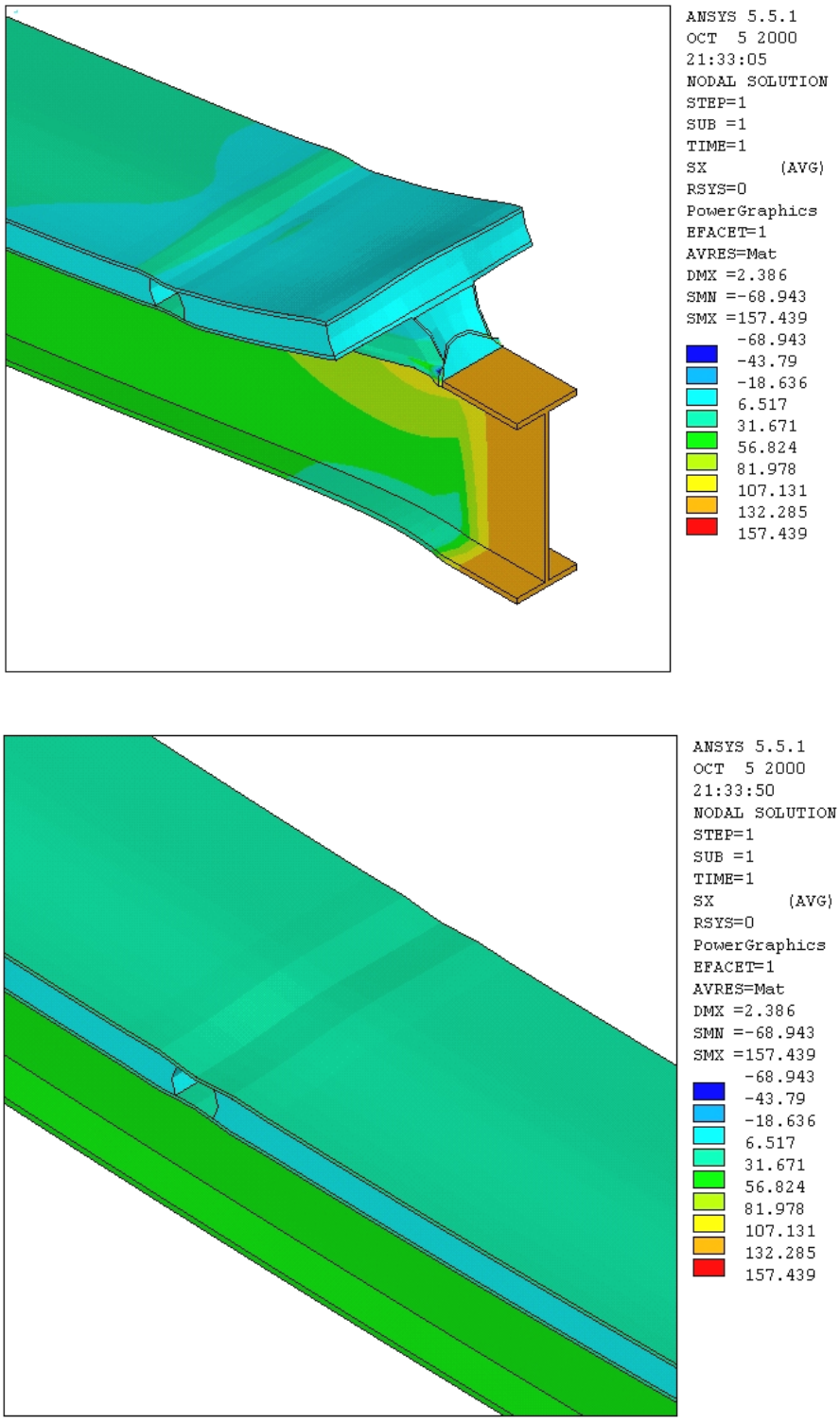

Figure 4.14: Plots of Bending Stress Due to a Decrease in Temperature

4.3.3 Non-Linear Analyses

A non-linear analysis was needed to calculate the displacements and strains associated with the contact elements and to determine how the forces were transferred from one surface to the other. The iterative method that provided the best method to calculate the contact elements was the Newton/Raphson Method.

The contact element stiffness, KN, was hard to predict. KN had to be large enough that it reasonably restrains the model from over-penetration, yet it should not be so large that it causes ill conditioning (ANSYS, 2000). ANSYS recommends using the following equation to calculate the normal stiffness:

$$KN = fEh \qquad (2)$$

where,

f is a contact compatibility factor between 0.01 and 100.
E is the Young's Modulus of the surface.
h is the length of the contact element.

The Young's Modulus of the FRP composite was 50000 MPa and the length of the contact element was approximately 0.1 mm, which was the physical gap between contact surfaces. Using these values, a range for KN of 50 to 500000 MPa was calculated. An iterative procedure was used to select a nominal value for KN that would lead to convergence. This value was determined to be 5000 MPa or less. Observing the stresses and strains from each analysis and recording the amount of processing time required for convergence, a KN of 1000 MPa was used for all sub model analyses.

There were four different submodel analyses conducted. The first and second analyses were conducted to determine the stresses and strains of the bolted connection closest to the

midspan of the bridge due to truck and thermal loading respectively. The third and forth analyses were conducted to determine the stresses and strains of the bolted connection closest to the supports due to truck and thermal loads respectively. From these four analyses, the behavior of the bolted connections and the interaction between the FRP composite saddle and deck with the existing steel girder could be determined.

4.3.3.1 Bolted Connection Closest to the Midspan

The first of the two analyses that was conducted was from the HS-25 truck loading. Figure 4.15 (top and bottom) shows a contour plot of the first principal stresses, which illustrates whether a portion of the model experiences tensile or compressive stress. The top contour plot illustrates the stresses of the entire submodel, whereas the bottom plot shows a smaller portion of the model without the elements of the bolted connection. The bottom plot shows relatively low stresses and provides a good estimate of stresses obtained from the main model under the same loading. The high stress in the top plot occurs where the bolts are connected to the steel plate on top. Because the method used to prestress the bolts did not provide accurate results at the ends of the bolts and only a correct clamping force, the stresses at the ends of the bolts should be neglected.

Figure 4.16 (top and bottom) shows a contour plot of the first principle stress of only the elements that comprise of the bolted connection (tube, plates, angles, clamp, etc.). In these two contour plots, the bolts where removed so that a better estimate of the stresses within the bolted connection could be obtained. From the upper plot, the highest stress is in the steel bar. The lower plot shows the stress in the steel clamp. The plot shows high tensile stress at the toe of the clamp where the steel clamp comes in contact with the underside of the top flange of the existing W-section. This is a result of bonding the clamp to the underside of the top flange, which was

required to maintain stability in the model. In the actual condition of the bridge, the clamp is not bonded to the W-section and tension would not develop. Therefore, the tensile stresses in the toe of the clamp should be ignored and only the compression stresses should be observed, which produces a stress approximately 63 MPa.

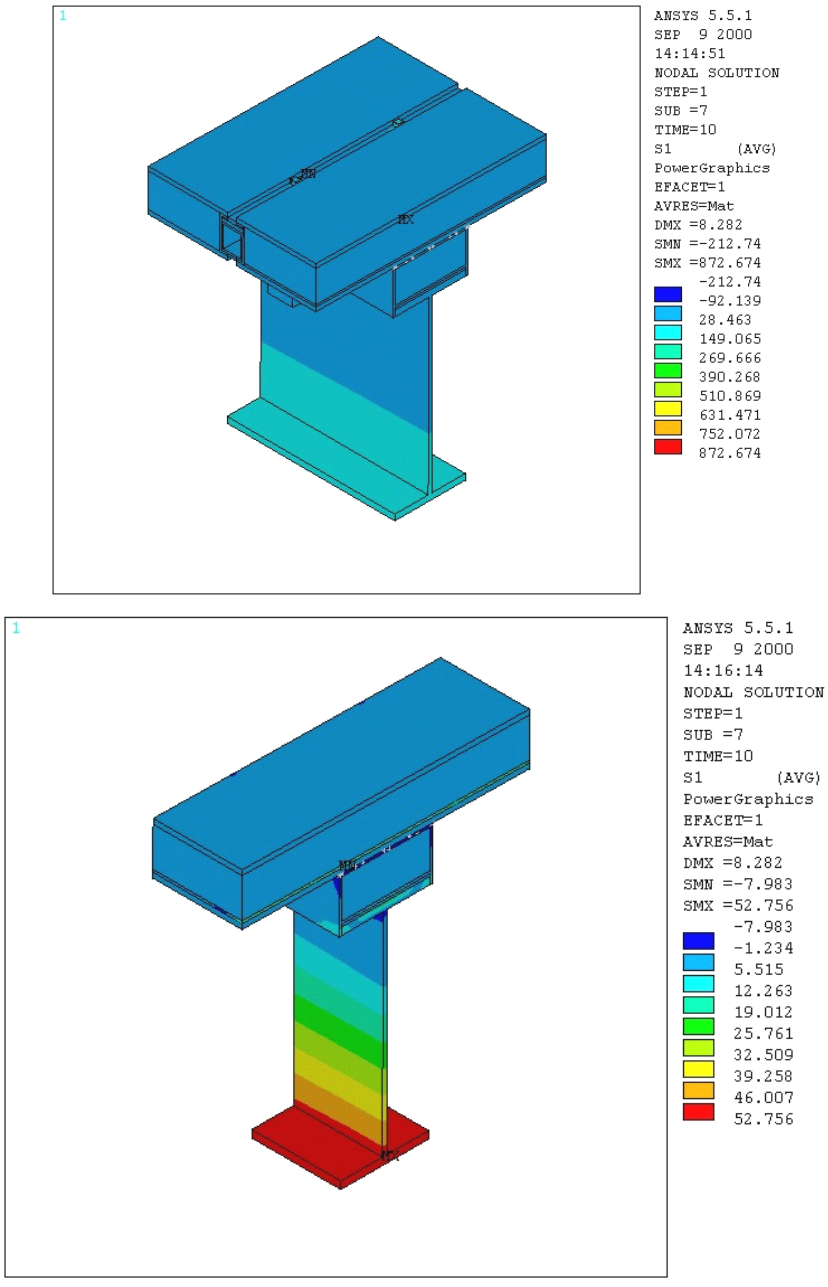

Figure 4.15 - Plots of First Principal Stress of the Submodel Closest to the Midspan under Truckloads

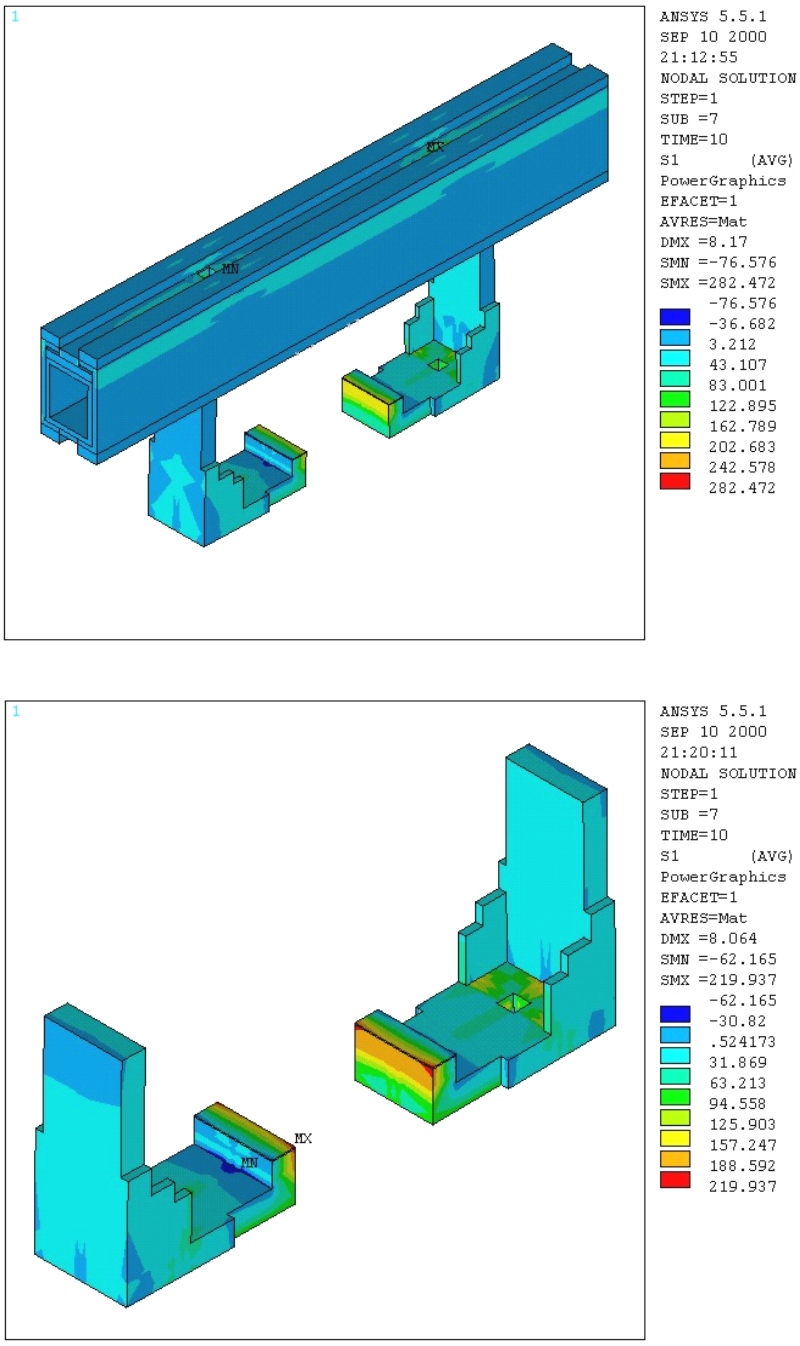

Figure 4.16: Plots of First Principal Stress of the Bolted Connection from the Submodel Closest to the Midspan under Truckloads

Plotting the Von Mises stresses shows a better estimate of the actual stress within the element (Section 4.3.2.1). The stress plot of the bolted connection around the bolthole with the

FRP composite tube, angles, and plate (Figure 4.17), shows the highest stress to be approximately 70 MPa, which is in the FRP composite bar at the location of the bolthole. The highest stress in this section is in the corners of the tube. Other noticeable stresses are in the steel bar at the bottom between the two FRP composite deck panels on each side. However, after neglecting the stress around the bolthole, the highest stress is in the order of 40 MPa.

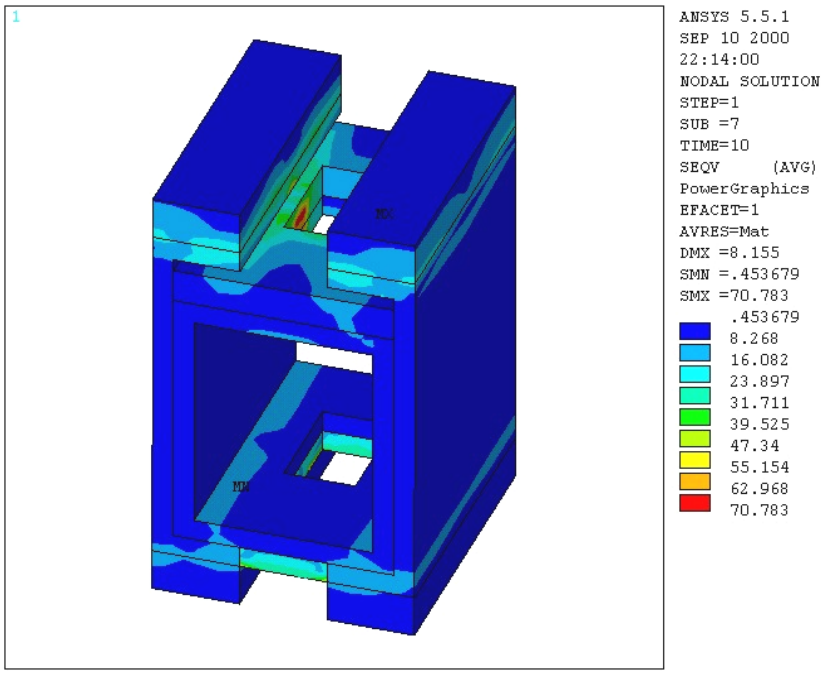

Figure 4.17: Plot of Von Mises Stress of the Bolted Connection Excluding the Steel Elements around the Bolt Hole

Figure 4.18 shows both the Von Mises stress (top) and first principal stresses (bottom) of a small portion between the two bolts. From these two plots, the deformations are caused by x-direction or bending stresses. These stresses are almost entirely compressive, with the highest stress in the steel plates at the top and bottom of the tube.

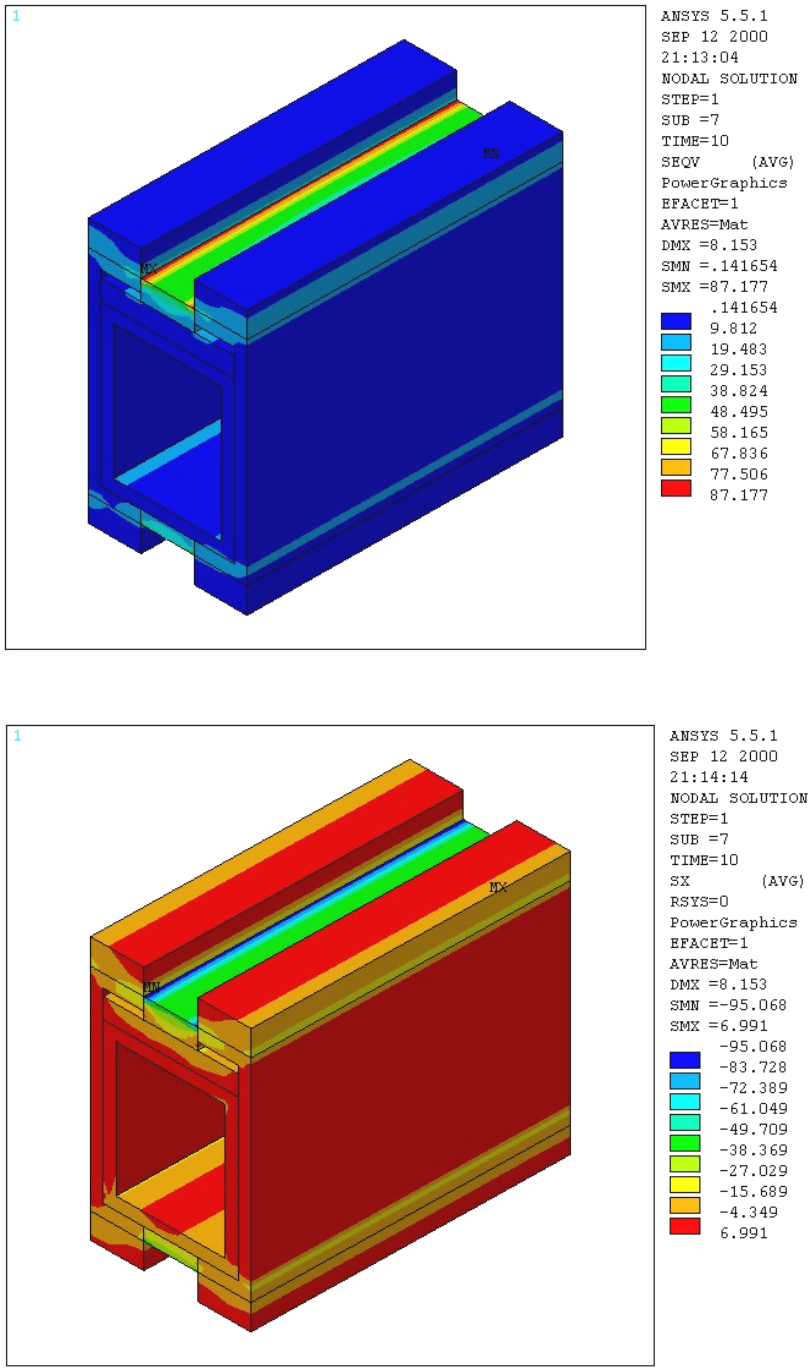

Figure 4.18: Plots of Von Mises Stress (Top) and Bending Stress (Bottom) of the Bolted Connection between the Bolts

Isolating the FRP composite tube and plotting the bending stress (Figure 4.19) shows the effect of the clamp force caused by the tightening of the bolt. The highest stress is

approximately 55 MPa. This plot also shows a small compression stress (25 MPa) in the FRP tube, which is a result of the section in bending.

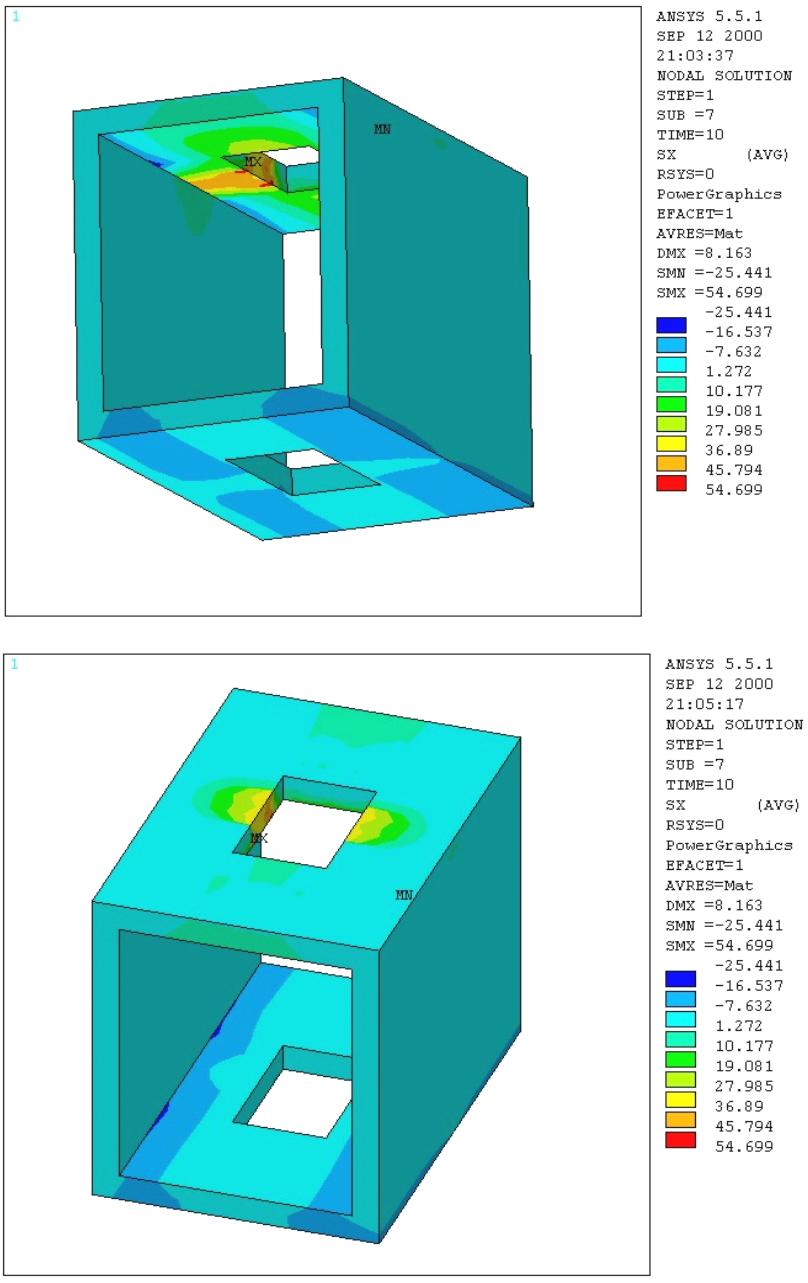

Figure 4.19: Plots of Bending Stress of the Pultruded Tube around the Bolt Hole

The second of the two analyses that were performed of the bolted connection closest to the midspan was from a positive temperature increase of 20 °C. Figure 4.20 shows two contour

plots of the first principal stresses. The positive thermal differential causes the materials to expand and the difference in thermal expansion between the steel and fiber composite is evident. The direction of expansion is restricted to only the vertical direction, because of the end restraints. This vertical expansion of the deck and saddle beam creates more tension in the bolts. The tension caused the heel of the steel clamp to rotate and displace vertically 0.5 mm. Not only does this expansion cause the heel to move, the top of the clamp slips 1 mm from the deck panel toward the center of the cross-section. The clamp develops tensile stress in the toe and should be neglect as discussed previously. Because the clamp is not actually bonded to the flange of the steel girder, more movement than calculated can take place. Even though the force within the bolt is not precisely known, there can be a correlation made between the stresses under truck and temperature loading cases. The stress appears to increase 20 to 25 MPa.

Isolating the connection elements and excluding the bolt elements, then plotting the first principal stresses (Figure 4.21, top) shows a higher compression stress within the clamp than from the first analysis (approximately 73 MPa). This is a result of the expansion from the fiber composite deck and saddle beam. Because the expansion is restricted to the vertical direction, compressive stress starts to become more evident within the steel bar on top of the connection. However, the compressive stress is relatively small with the highest, approximately 25 MPa (Figure 4.21, bottom).

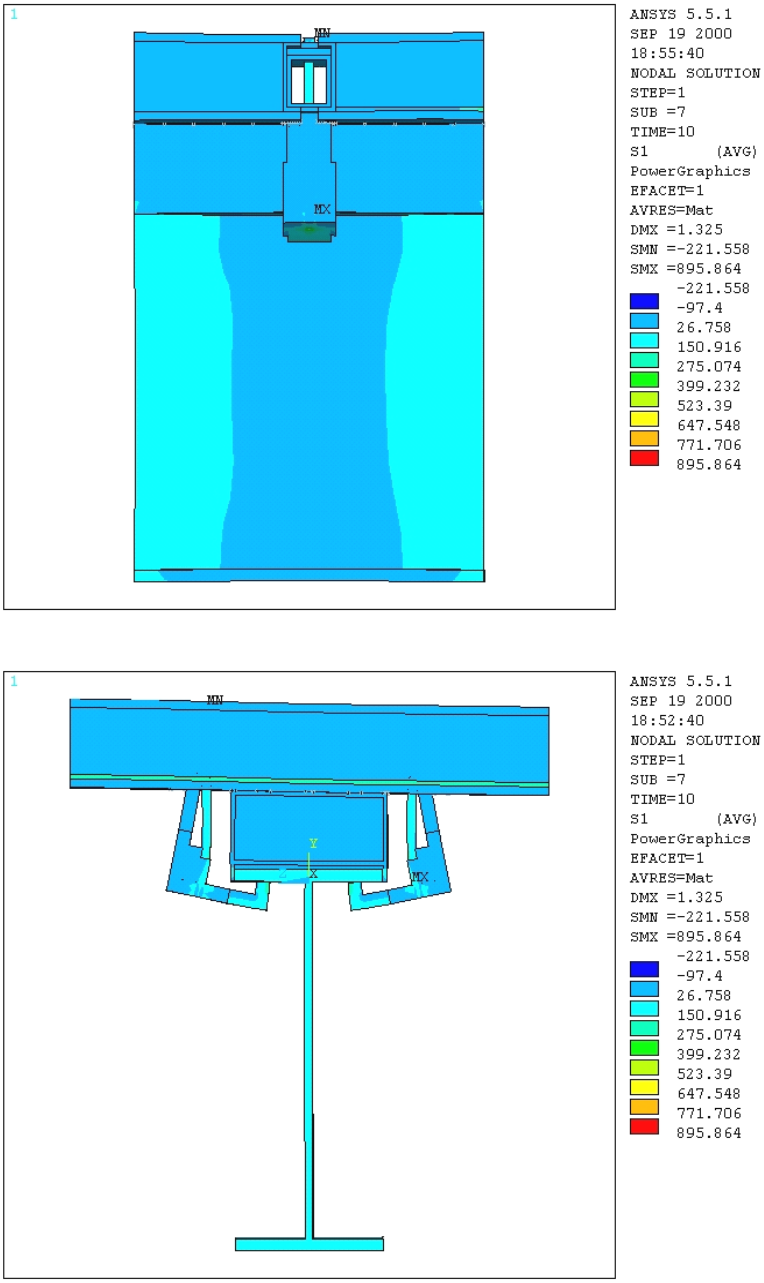

Figure 4.20: Plots of First Principal Stress of the Submodel Closest to the Midspan under Temperature Loading

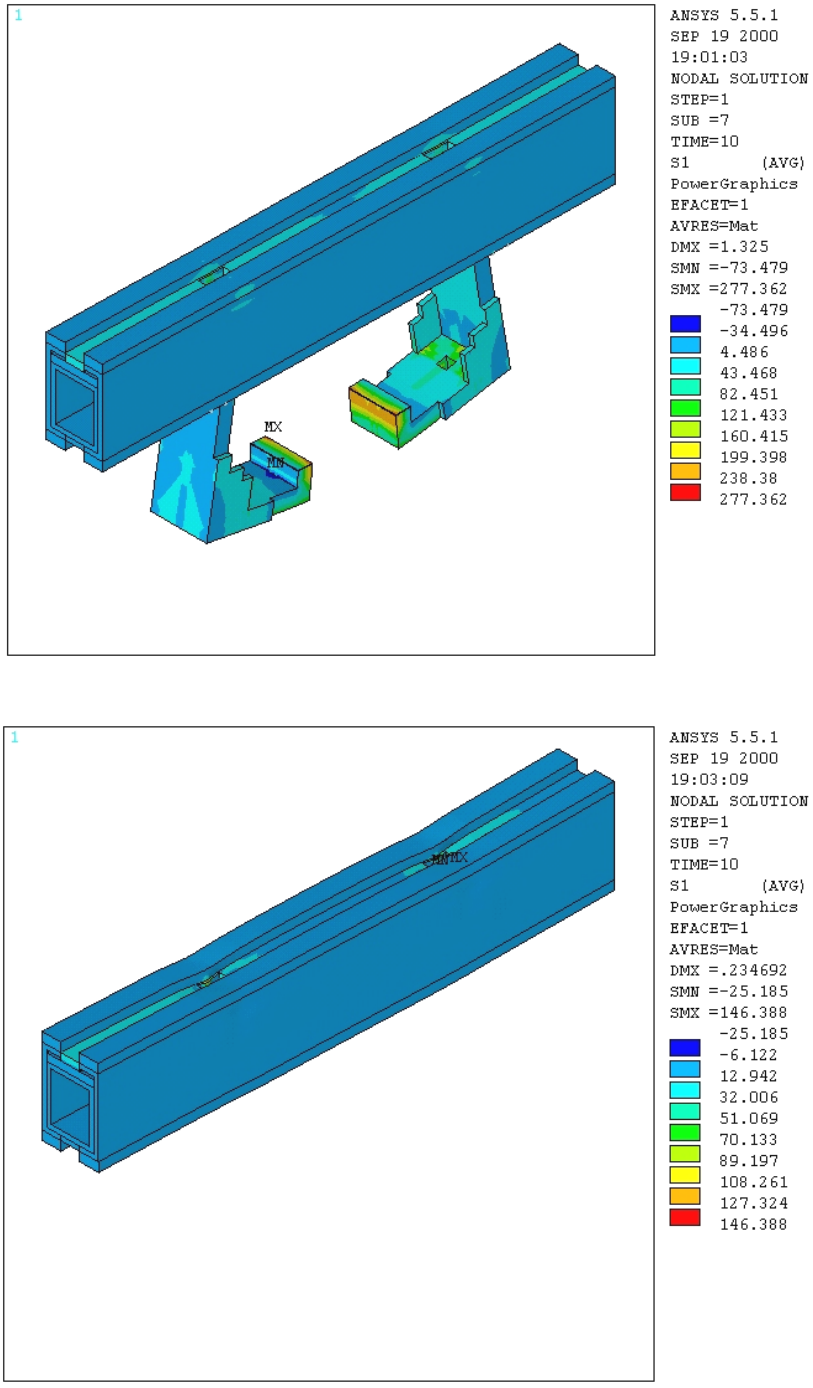

Figure 4.21: Plots of First Principal Stress of the Bolted Connection under Temperature Loading

4.3.3.2 Bolted Connection Closest to the Support

The first of the two analyses that was conducted was from the HS-25 truck loading. Figure 4.22 shows a contour plot of the first principal stresses. The top contour plot shows the stress from the side, whereas the bottom plot shows the stress from a sectional view. The top plot shows a kink in the deflection of the FRP composite deck and saddle beam at the locations of the steel clamp. This could be attributed to the FRP composite deck and saddle beam not having enough fixity at the supports, which allows it to rotate. This rotation causes the deck and saddle beam to lift from the steel girder. The lift of the FRP saddle beam and deck causes the steel clamp to deform upward (bottom plot).

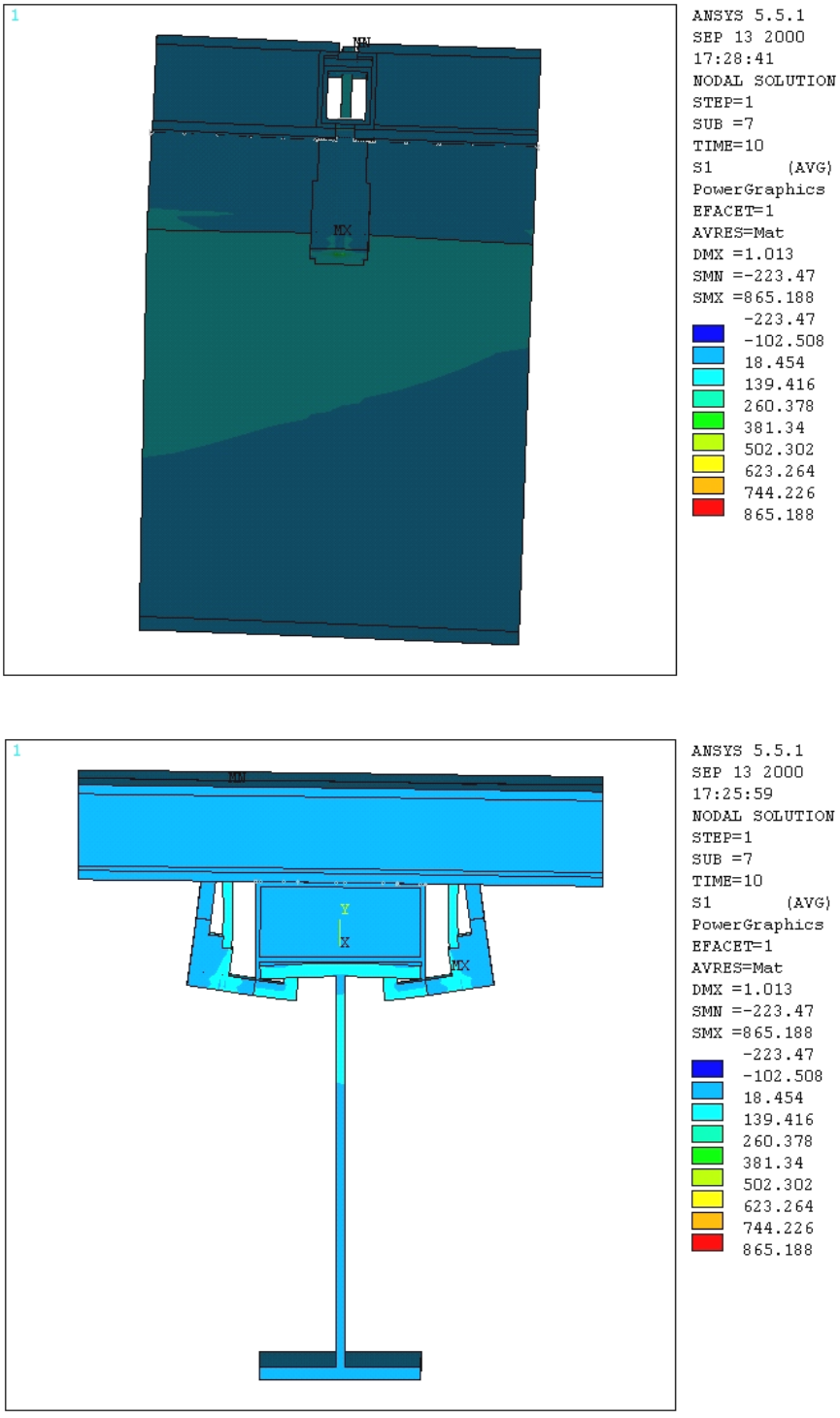

Figure 4.22: Plot of First Principal Stress of the Submodel Closest to the Supports under Truckloads

Isolating the connection elements and excluding the bolt elements, (Figure 4.23) shows the first principal stresses. The stresses are lower than the stresses of the bolted connection at the midspan. However, the results from the thermal loading are similar in both locations.

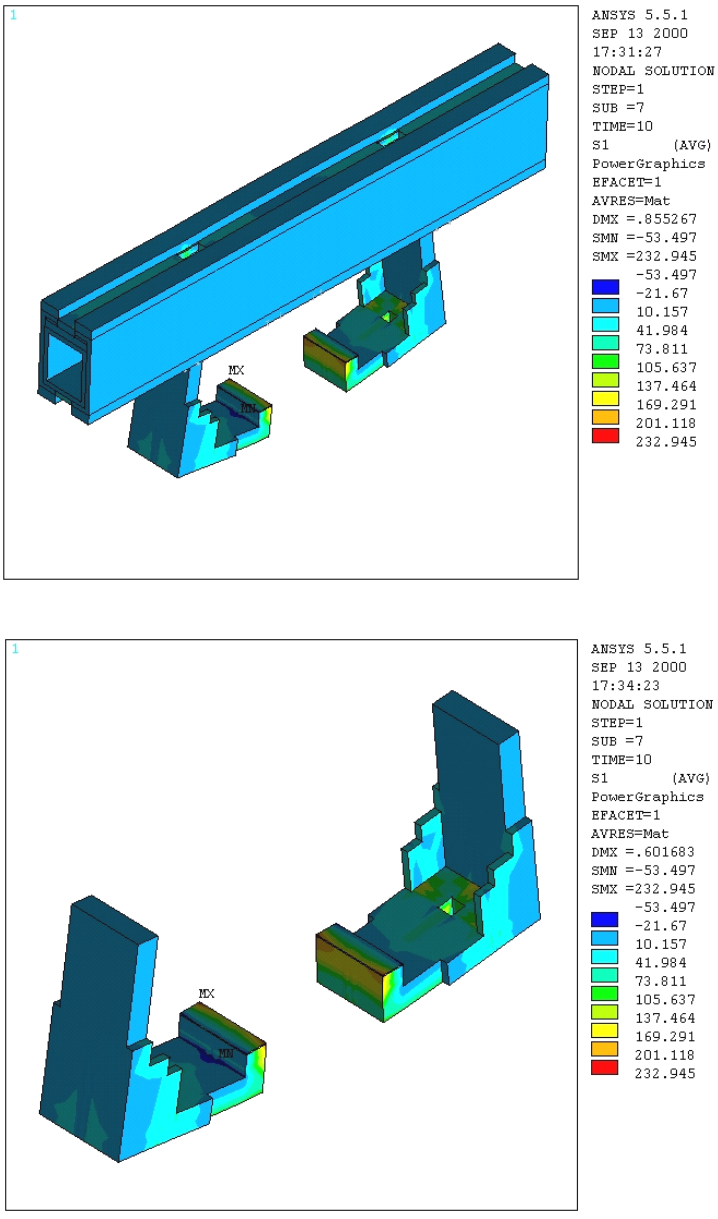

Figure 4.23: Plots of First Principal Stress of the Bolted Connection from the Submodel Closest to the Supports under Truckloads

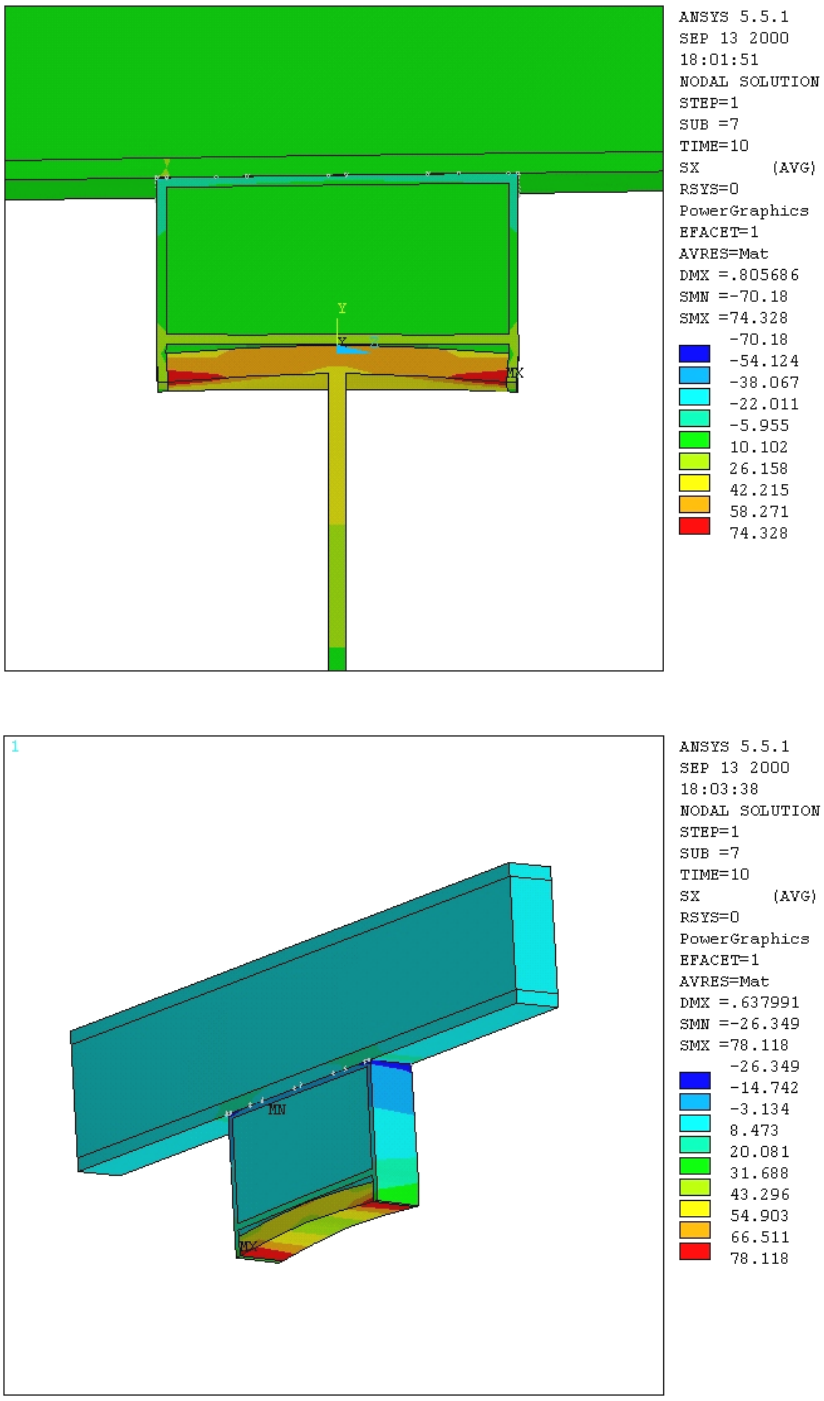

Figure 4.24: Plots of Bending Stress of the Submodel Closest to the Supports

Figure 4.24 illustrates how the steel girder, FRP saddle beam and deck undergo deformation at the end of the submodel closest to the support. The FRP saddle beam and deck

deform differently than that of the steel girder. This is attributed to the fixity of the steel girder. In both plots, the stress in the FRP composite elements is small, under 30 MPa, and shows very little stress in the FRP deck. This shows that the majority of the bending stress is within the steel girder.

A closer look at the connection elements with one plot of the Von Mises stress around the bolt (Figure 4.25, top) and another plot between the bolts (Figure 4.25, bottom) show no significant high stresses. The highest stress is around the bolthole.

4.4 Summary

Chapter 4 discussed the three types of analyses that were performed: a modal analysis, static analysis, and non-linear analysis. The modal analyses provided the modes and frequencies of vibration as well as how the steel girder and FRP composite deck absorbed energy under dynamic loading. The static analysis provided a desirable way to determine the stresses, strains, and displacements within the main finite element model. The non-linear analysis provided an accurate method to calculate the contact elements, and the interaction between the steel girder and FRP composites.

Chapter 4 discussed the accuracy of the finite element models, by comparing the results of the main model to the results from non-destructive testing previously performed on the bridge. The difference in stress was between 4 and 12 percent.

Chapter 4 discussed the frequencies obtained from non-destructive testing and how it compared to a computer analysis. The frequencies of the deck and girder collected from NDT of the bridge showed differences in energy dissipation. The data from the non-destructive testing showed that the FRP deck absorbed energy evenly over a broad range of frequencies, whereas the steel girder absorbed energy at a smaller range of frequencies, which was lower. The results

from the modal analysis that was performed using ANSYS, provided information on primary mode shapes and their frequencies.

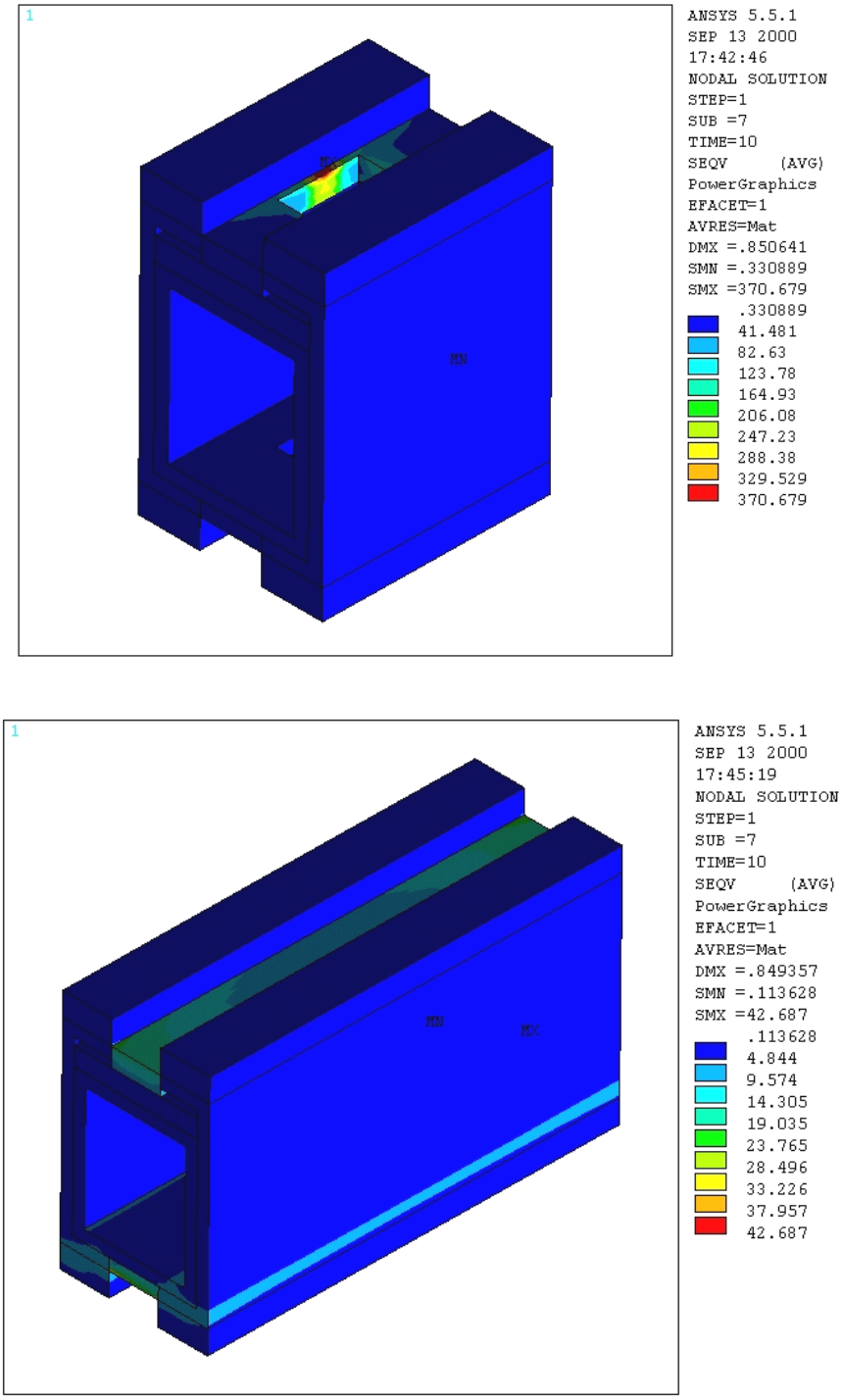

Figure 4.25: Plots of Von Mises Stress of the Bolted Connection of the Submodel Closest to the Supports

Chapter 4 discussed the analyses of the main finite element model. From the analyses, the highest stresses were found to be at the bolted connections closest to the midspan and to the supports. These were important in determining where the submodels would be defined. From the truckloads, the strength of the bridge was observed to determine whether or not composite action had developed.

Lastly, Chapter 4 discussed the analyses of the sub finite element models. From the analyses, the stresses were recorded and observed so that an assessment could be made as to the long-term behavior of the bridge. Certain issues concerning the way the bolts were prestressed were discussed, such as:

- Applying a temperature change on the bolt elements.
- Applying a prestress force equal and opposite within the bolts.

The temperature analysis used to prestress the bolts provided the correct stress at the center of the bolts, and a much higher incorrect stress toward the end constraints. The second analysis calculated the desirable stress at the point of the load, but increased toward the constraints and decreased toward the middle of the bolts. Both analyses provided the desirable displacements at the ends that would provide the clamping force in the model. For the submodel analyses, the temperature loading was chosen, and the stresses within the bolts were neglected.

Chapter 5

Results

5.1 Introduction

The primary goal of the finite element analyses and non-destructive testing was to help locate any areas on the bridge that might develop problems due to overstressing, excessive vibration, or deterioration. Because the allotted time of this study would not allow laboratory testing for fatigue and environmental deterioration, the assessment was based on interpretation of the finite element models. The purpose of the finite element models was to determine the stresses and strains induced by truck and thermal loads. Close examination of these stresses and strains helped to identify areas of concern that might lead to long-term behavior problems. The effects of vibration on the bridge could not be determined from the finite elements models. However, identifying modes and frequencies of vibration help to identify if problems could exist by comparing the frequencies calculated to a predetermined frequency range that could cause problems (i.e. frequency ranges specified in AASHTO).

In the original scope of this study, there were several concerns to be addressed.

- **Composite action**: KDOT redesigned the bridge using the combination of four innovations: the FRP composite saddle beams, the polymer concrete overlay, the FRP composite honeycomb deck panels, and the bolted connection. The combination of these four innovations had not previously been implemented into a structure and the behavior of this combination of innovations had not been studied in detail. When KDOT began to redesign the bridge, the amount of composite action that developed between the FRP composites and the steel girder was not known. KDOT wanted to know if composite action developed between

the steel girder and FRP composites, and if so, how much composite action is developing.

- **Vibration**: Identifying the primary mode shapes and the associated frequencies help to identify the condition of the bridge and allow estimates to be made on the effects of excessive vibration. In some cases, excess vibration may lead to fatigue problems in the bolted connection and/or speed up deterioration of the bridge. Excessive vibration may weaken connections and require frequent maintenance. KDOT was concerned about the vibration and was curious about the vibration patterns of the bridge.
- **Connections**: Another concern KDOT had was in the behavior of the lightweight FRP composites with the rigid steel girders. KDOT wanted to know how well the two materials performed together, and if the FRP composites were durable enough to withstand continuous traffic loading. Because FRP composites pose problems in connectivity, KDOT was interested in the effectiveness of the designed connection of the FRP saddle beam and FRP deck panel to the steel girder.

5.2 Composite Action

The bolted connection of the FRP deck to the steel girder is the main component contributing to the development of composite action. Without something bonding the three main components together, either by friction provided by the steel clamp or with an adhesive to transfer the transverse shear from one component to the other, composite action could not exist. The main FE model was used for two reasons; to generate the displacements for each submodel, and to model the behavior of a completely bonded system to determine the maximum composite action that could develop. The submodels were mainly used to determine the interaction between the three main components as it was originally designed, and provide stresses and strain within the bolted connection. An interpretation of both the main FE model and sub FE models would

provide valuable information to determine if composite action could develop, how much developed, and how much of the deck (i.e. effective width) contributed to the capacity of the bridge.

Two analyses were performed to predict if composite action developed, and to determine how much strength would be gained with the addition of the FRP saddle beam and deck panels. Figure 5.1 (top) shows the result of the first analysis, which consisted of only the existing steel girder under AASHTO HS-25 truckloads. The second analysis (Figure 5.1, bottom) consisted of the main model under the same loads, which included the FRP saddle beam and FRP deck panel. With these two analyses, the bending stress could be observed. From Figure 5.1 (top) the maximum bending stress at the mid span of the beam was approximately 67 MPa. From the main model analysis (Figure 5.1, bottom), the maximum bending stress at the mid span was approximately 48 MPa. Therefore, if the bridge were bonded the stress could decrease as much as 28%.

$$\text{Percentage of stress decreased} = \frac{67MPa - 48MPa}{67MPa} * 100\% = 28\%$$

Because the section is not bonded throughout the entire bridge, a 28% decrease in stress is not feasible. However, observing the bending stress in the top flange of the FRP deck of the bonded system shows only a portion contributing. Figure 4.10 shows the stresses at the top and bottom of the FRP deck. The upper figure provides the stresses at the top of the FRP deck and shows an effective contributing flange width of approximately 200 millimeters, which is approximately the same width as the steel girder. The lower figure provides evidence that the stresses are being transferred from the FRP saddle beam into the FRP deck. Figure 5.2 shows the bending stress at the bottom of the FRP deck from the submodels. From this figure it is not as evident that the

stresses are being transferred, which suggests that the bolted connection does not provide enough force to adequately transfer all the transverse shear. Although it is evident that some of the shear is transferred, it would not be the case at the locations were the bolted connections are not installed. Therefore, the bolted connections will add very little to resist the transverse shear caused by composite action and should be neglected.

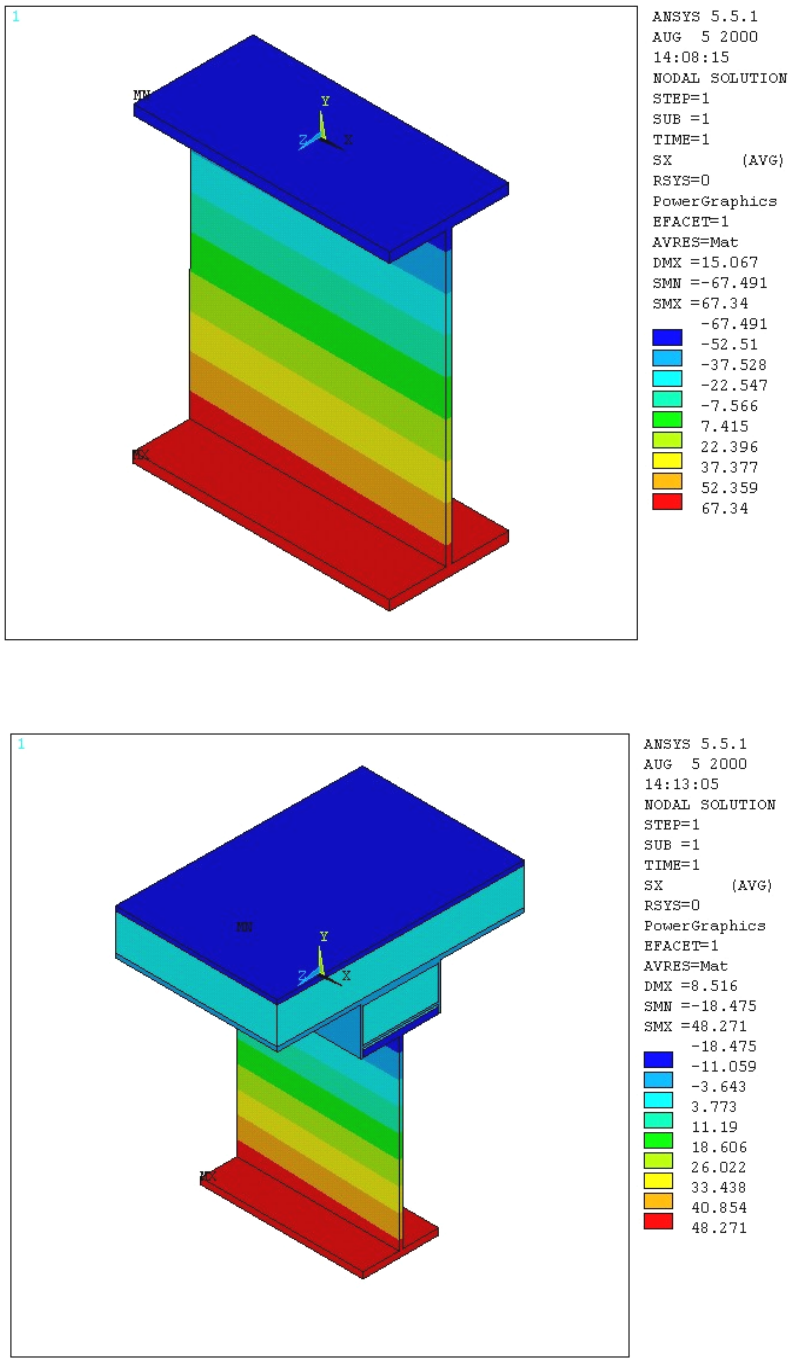

Figure 5.1: Plots of Bending Stress at the Midspan of the Bridge with All of the Components (Bottom) and of Just the Existing Steel Girder (Top)

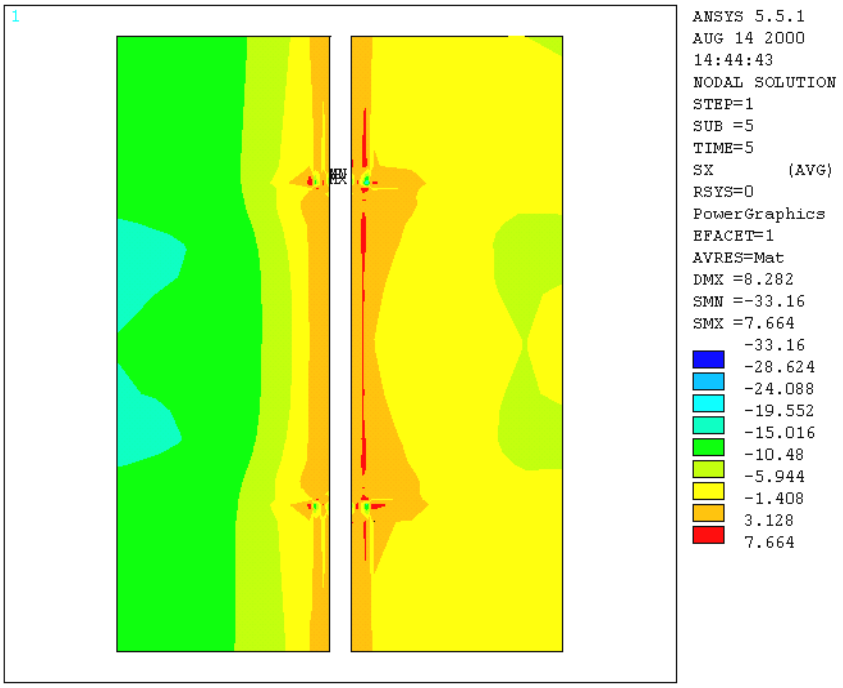

Figure 5.2: Plot of Bending Stress from the Sub Model of the Surface between the Saddle Beam and Deck

5.3 Vibration

The modal analyses provided useful data on how the fiber composites and steel girder behaved together. Figures 4.1 through 4.4 show a mechanism for dissipating energy caused by traffic loads by the FRP deck and steel girder. The spectral analysis provided by the non-destructive testing provided a method to identify how the two materials absorbed energy. The steel girder dissipated energy at significantly lower frequencies than the FRP deck. The differences can be directly correlated to the stiffness of each material and the mass associated with each material. Because the FRP deck is light weight and less stiff (i.e. the Young's Modulus and moment of inertia of the FRP composites compared to those of the steel girder) compared to the steel girder, the frequencies are higher. This difference in dissipation of energy suggests that the two

components behave independently, which makes it improbable that composite action would develop.

The inability of the FRP composite deck to dissipate the energy in a smaller range of frequencies could lead to deterioration problems. Although the magnitude of the stress is below the ultimate strength of the bridge, excessive vibration could create problems for the bolted connections. These problems include cracking of the deck overlay, loosening of the bolted connections, and long-term fatigue or deterioration problems. In particular, the bolted connections should be monitored because of the concerns addressed in the temperature and static analyses described below.

5.4 Connections

To predict the long-term behavior of the bridge, an assessment of the stresses from the submodels had to be made.

The analysis of the first submodel under truckloads does not show any significant stresses that could lead to long-term problems. The stresses within the steel elements are less than 100 MPa, which is less than 40 percent of the yield stress. The stresses within the FRP composite elements are even smaller with the largest being approximately 60 MPa. Under normal loading the bridge should not experience any high stresses that would lead to strength problems. However, the combination of the thermal loads and truckloads could lead to higher stresses within the components of the bolted connection. This may cause sufficient stresses to fatigue the material or deteriorate over time. If the temperature decreases 20 °C or more over a short period of time and is heavily loaded with trucks, the bolted connections could become overstressed. The effect of decreasing the temperature also could create problems in the bolted connections. Depending on the actual pretensioning force in the bolts, the shrinkage of the FRP deck and

saddle beam due to decrease in temperature may relieve some of the clamping force. Under dynamic loads, such as traffic loading, these components could move, and the surfaces could wear and deteriorate. If the components are allowed to slide with respect to each other and the tightness of the bolts relax, the connections could fail to function as designed.

The analysis of the bolted connection closest to the supports revealed several possible long-term problems. These problems would be instigated by the different support conditions between the FRP deck and the steel girder. Because the steel girder is fixed in the abutments and the FRP deck is free to rotate, additional strain develops in the bolted connection. The force to keep the deck and saddle beam clamped to the steel girder may cause cracking in the deck overlay, because this will allow tension to develop due to negative bending and tension in the top of the FRP deck. The concrete deck overlay needs to have a large enough tensile strength to withstand this stress. Cracking has already been noted in the bridge and may be a result of these stresses. The role of the polymer concrete is to protect the fiber composite elements from the environmental elements such as ultraviolet rays, dirt, and moisture. As a result of the polymer concrete cracking, the connection elements could weaken and function abnormally. This could lead to deterioration and long-term effects that would hinder the performance of the bridge. The indications of long-term behavior problems in the target bridges could be more significant for bridges having longer spans. If the steel girders were embedded into abutments similar to the FRP composite bridges in this study, the clamping force would need to be increased to hold the deck and saddle beam. A simple solution would be to release the moment at the ends of the girder.

These particular cases are based on a static analysis of the bridge. The influence of a long duration of vibration and environmental weathering can have a negative impact on the

bridge when combined with traffic loads. However, the complete impact of these effects could not be determined within the scope of this study.

5.5 Summary

Chapter 5 described an analysis of the steel girder under truckloads and an analysis of the steel girder with the FRP deck and saddle beam under truckloads to determine how much strength was gained. If the FRP saddle beam and deck were bonded to the girder, the stress in the bottom fiber of the girder could be decreased by 28 percent. However, from modal testing and the submodel analyses, only small amounts of composite action are exhibited. The modal test showed two different spectrum patterns of dissipating energy, which suggests that the FRP composite deck and steel girder do not behave as a composite system. A contour plot of the bending stress of the bottom of the FRP deck shows little stress variation at the surface were the saddle beam is located, which suggests that very little shear is getting transferred.

Chapter 5 discussed the effects of vibration and how the different materials and components behaved together. From the non-destructive evaluation conducted using accelerometers, the energy absorbed within the deck was at a significantly higher frequency then the steel girder. This is due to the lightweight and the lower modulus of elasticity of the fiber composites. A higher frequency of vibration also increases the number of cycles based on stress reversal. This tendency can lead to long-term problems.

Lastly, chapter 5 discussed the performance of the bolted connections. Under steady state truck loads, the connection toward the midspan does not experience any significant high stresses that would warrant problems. However, the combination of truckloads, temperature, and vibration could lead to long-term problems of the bolted connections closest to the supports.

Chapter 6

Implementation Plan

6.1 Introduction

In this chapter, the structural monitoring technique chosen for evaluating the FRP composite bridge is discussed. This chapter also will have a detailed implementation plan showing the location of the instrumentation.

6.2 Structural Monitoring Techniques

Several monitoring techniques are recommended to evaluate the long-term behavior of the two bridges in the areas of concern documented in this report. There are three monitoring and evaluation techniques that are recommended to evaluate the two bridges:

- Visual inspection.
- Continuous monitoring.
- Non-destructive testing.

Visual inspection is recommended at all of the bolted connections closest to the supports as well as continuous monitoring of temperature and strain of these same locations. It also is recommended that non-destructive testing be used on the bridge yearly or bi-yearly to evaluate the performance of the FRP deck. Specifics of these techniques are described below.

1. **Visual Inspection**: There are concerns with the performance of the bridge that cannot be monitored with sensors and will require visual inspection. These include:
    - Visual inspection of the polymer concrete overlay to detect if there is any deterioration or cracking.

- Visual inspection of the underside of the deck where the clamps are bearing. Specific concerns include wear caused by the clamp slipping or grinding.

2. **Continuous Monitoring**: To evaluate the combined effects of temperature differentials and traffic loading conditions, it is recommended that a continuous monitoring system be installed at one of the bridges. Continuous monitoring requires equipment to be installed on the site in an area where vandalism and obstruction will not occur. The continuous monitoring technique should consist of the following:

    - Strain sensors placed near the bolted connections closest to the supports.
    - Temperature sensors placed next to the strain gages.
    - Mechanical box so that the measurements can be collected and sent via modem.
    - The temperature and strain should be measured once a week at the same time and vicinity so that the two measurements can be correlated.

3. **Non-destructive Evaluation**: The long-term performance of the FRP deck is difficult to measure. Under normal temperature and traffic loads, the FRP deck does not appear to experience stresses that would warrant concern. However, the effect of excessive vibration is a concern, and it is recommended that acoustic emission testing be performed yearly or bi-yearly so that an assessment of the FRP deck can be made. Areas of the FRP composite bridge to examine are:
    - Underneath the FRP composite deck nearest the abutments.
    - Underneath the FRP composite deck at the midspan.

The three recommended monitoring and evaluation methodologies will provide an assessment of the FRP composite bridges and will help to identify any problems. The following section describes the implementation of the sensors and their relative location.

6.3 Implementation Plan

Figure 6.1 shows the implementation plan of instrumentation for the bridge. The strain and temperature sensors should be permanently bonded near the bolted connections closest to the supports. These sensors will continuously monitor the bridge and the measurements will be collected in a database within a mechanical box on site (Figure 6.2 and 6.3). This data will then be transferred via modem or LAN to a desired location. The acoustic emission sensors can be temporarily bonded or permanently bonded to the FRP deck near the bolted connections closest to the supports. These sensors will be used yearly or bi-yearly with non-destructive testing. The AE sensors should be midway between the steel girders and far enough from the bolts so that accurate results can be obtained (Section 2.3.5.5).

6.4 Summary

Chapter 6 discussed the techniques recommended to evaluate the long-term behavior of the KDOT FRP composite bridges in Crawford County. The implementation plan illustrated the ideal locations for the sensors and equipment.

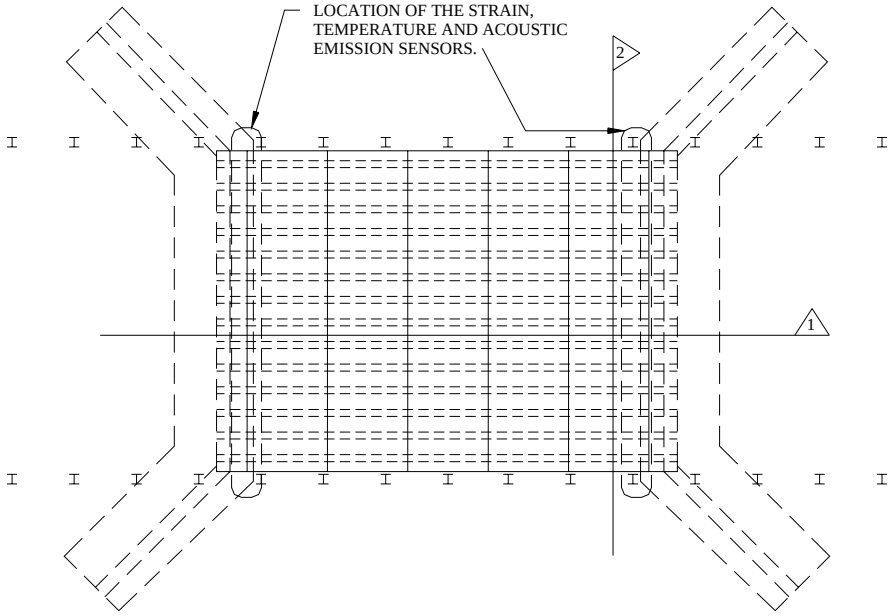

Figure 6.1: Instrumentation Plan/Layout

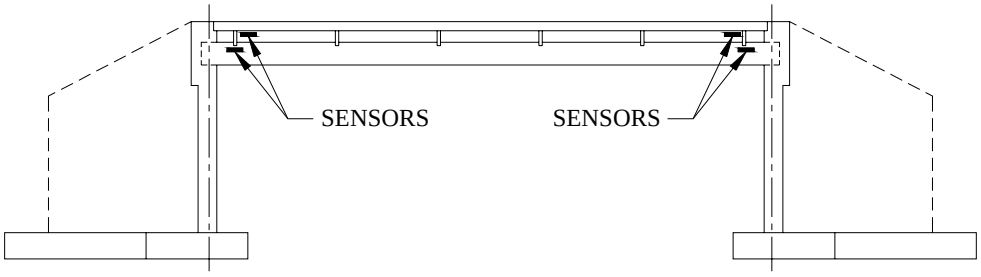

Figure 6.2: Section 1 of the Instrumentation Plan/Layout

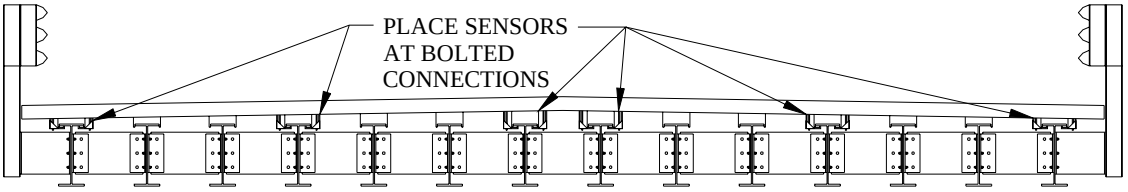

Figure 6.3: Section 2 of the Instrumentation Plan/Layout

REFERENCES

Chang, Fu-Kou, "Structural Health Monitoring: 2000," A Technomic Publication, 1999.

Collins, G.L., Corporation, http://www.lvdtcollins.com/, 1997.

Hauptmann, P., "Sensors: Principles and Applications," Carl Hanser Verlag, Prentice hall, 1991.

Jones, B. E., "Current Advances in Sensors", The Adam Higer Series on Sensors, 1987.

Measures, R. M., K. Liu, M. Leblanc, K. McEwen, K. Shankar, R. C. Tennyson, and S. Ferguson, "Damage Assessment in Composites with Embedded Optical Fiber Sensors," University of Toronto Institute for Aerospace Studies, 1991.

Moore, R. L., "Basic Instrumentation Lecture Notes and Study Guide," Instrument Society of America, 1976.

Moseley, P. T., and A. J. Crocker, "Sensor Materials," Institute of Physics Publishing Bristol and Philadelphia, 1996.

Non Destructive Testing Association, http://www.winzurf.co.nz/, 1996.

Schreiner, J. and B. Michael, "Lateral Distribution in Kansas DOT Steel Girder Bridge with FRP Deck," University of Missouri, Columbia.

Sikorsky, C., "Development of a Health Monitoring System for Civil Structures Using a Level IV Non-Destructive Damage Evaluation Method," Chang, Fu-Kou, editor, "Structural Health Monitoring: 2000," A Technomic Publication, 1999.

Solomon, S., "Sensors Handbook," McGraw Hill, 1999.

Todd, M. D., C. C. Chang, G. A. Johnson, S. T. Vohra, J. W. Pate, and R. L. Idriss, "Bridge Monitoring Using a 64-Channel Fiber Bragg Grating System," 1998.

Udd, E., "Applications of Fiber Optic Smart Structures," Optics & Photonics News, 1996.

Varadan, V. K., and V. V. Varadan, "Wireless Remotely Readable and Programmable Microsensors and MEMS for Health Monitoring of Aircraft Structures," Chang, Fu-Kou, editor, "Structural Health Monitoring: 2000," A Technomic Publication, 1999.